Applied Ocean Research 129 (2022) 103367

Contents lists available at ScienceDirect

Applied Ocean Research

journal homepage: www.elsevier.com/locate/apor

Simultaneous sea state estimation and transfer function tuning using a network of dynamically positioned ships

Raphaël E.G. Mounet [a,b,*], Ulrik D. Nielsen [a,b], Astrid H. Brodtkorb [b], Eduardo A. Tannuri [c], Pedro C. de Mello [c]

[a] DTU Civil and Mechanical Engineering, Technical University of Denmark, DK-2800 Kgs., Lyngby, Denmark
[b] Centre for Autonomous Marine Operations and Systems, NTNU AMOS, NO-7052, Trondheim, Norway
[c] Numerical Offshore Tank, TPN-USP, Universidade de São Paulo (USP), SP, Brazil

ARTICLE INFO

Keywords:
Wave spectrum estimation
Network of ships
Dynamic positioning
Measured ship motions
Transfer function tuning
Data fusion

ABSTRACT

This paper presents a study focused on wave spectrum estimation in practical scenarios where multiple ships operate in the same geographical area, potentially forming a network of wave recorders. A novel methodology is proposed to improve the accuracy and precision of the wave spectrum estimates, by combining sea state estimation methods and techniques for tuning the wave-to-motion transfer functions. The framework of the wave buoy analogy is used to derive estimates for each ship through the use of measured ship motion data and available initial estimates of transfer functions. Simultaneously, the wave-to-motion transfer functions of the individual ship are tuned by utilizing a weighted version of the wave data inferred on board the other ships in the network. The overall architecture of the procedure is modular, in the sense that various approaches may be implemented for obtaining sea state estimates and tuned transfer functions. The methodology is demonstrated through two case studies, one based on simulated vessel responses, and the other using model test data of ship motions in a wave tank. Both case studies consider a network of three ships in long-crested waves equipped with a dynamic positioning system. It is shown that the procedure provides good wave spectrum estimates, and leads to reduced uncertainty in the estimates via tuning of the vessel transfer functions.

1. Introduction

Sea state estimation (SSE) refers to an ensemble of methods and techniques used to characterize the properties of the sea-surface wave at a given time and position. The ocean waves represent the most important (compromising) met-ocean phenomenon for ships and offshore structures, as most of these structures are dominated by wave loads, with impacts on safety and fuel efficiency (Bitner-Gregersen et al., 2014). The scarcity of in-situ wave data from vast areas of the world's oceans is yet an ongoing problem. Enhancing safety and efficiency at sea through quantification and mitigation of the inherent uncertainties to environmental description is increasingly recognized by the shipping, offshore and renewable energy industries, as well as in coastal engineering. In the framework of estimation theory, collecting more information about a considered quantity is one way to reduce the epistemic (knowledge-based) uncertainty; the other way is to improve the models and methods of estimation (Bitner-Gregersen et al., 2014).

Advanced automatic control of vessels in varying weather and changing operational conditions, via the use of *dynamic positioning* (DP) systems, requires computationally efficient algorithms to estimate the sea state parameters with frequent updates, e.g. Brodtkorb et al. (2018a,b). In steady-state DP operations, the reliability and accuracy of the estimates are even more important. On the other hand, installation and maintenance of offshore marine units can also require several construction vessels to operate in DP on the same site, where for safety reasons, it is beneficial for the operators to work with available real-time in-situ estimates – as well as predictions – of the encountered wave systems. The technology for communication of data at sea is becoming better, enabling sharing of information about the sea state within a fleet of vessels (Nielsen et al., 2019). Emerging network-based approaches facilitate collaboration between adjacent vessels, to bring more timely information and improve the situational awareness of the control systems and (remote) operator. Beyond conventional ships, this is particularly relevant for the missions of small unmanned surface vehicles (USVs) (Dallolio et al., 2021), where the awareness of the wave environment as well as the fidelity of the vessel hydrodynamic model play an essential role.

The study of wave-ship interactions in the linear theory typically relies on the knowledge of high-fidelity complex-valued transfer functions

* Corresponding author at: DTU Civil and Mechanical Engineering, Technical University of Denmark, DK-2800 Kgs., Lyngby, Denmark.
E-mail address: regmo@dtu.dk (R.E.G. Mounet).

https://doi.org/10.1016/j.apor.2022.103367
Received 17 May 2022; Received in revised form 12 September 2022; Accepted 1 October 2022
Available online 13 October 2022

(TRFs), expressed in the frequency domain, and relating mathematically the wave and ship response spectra (St. Denis and Pierson Jr., 1953). In the literature, the amplitude of a wave-to-motion TRF is commonly named the *Response Amplitude Operator* (RAO). The RAOs, as functions of wave direction and wave frequency, are estimated for a ship in a seaway for given operational conditions and hull geometry description, thus depending on the draught – varying with the loading conditions – and forward speed. They can be computed through the equations of motion of the ship, for instance, based on potential flow theory or closed-form solutions (e.g. Salvesen et al., 1971; Lloyd, 1998; Jensen, 2001; Jensen et al., 2004).

The principle of the so-called *wave buoy analogy* (WBA) is to consider the ship as a sailing wave buoy. The inertial and navigational sensors already installed on board most marine vessels – namely, the IMU and GPS – can be used to derive an estimate of the waves inducing the measured responses. There exist many different SSE methods based on measured vessel responses; a comprehensive account is given in Nielsen (2017). In general, two main frequency-domain methods have been developed to estimate the on-site directional wave spectrum based on ship response measurements: (1) parametric methods which assume the wave spectrum to be composed of parameterized wave spectra, e.g. Montazeri (2016); and (2) non-parametric methods, where the values of the directional wave spectrum are recovered in a completely discretized frequency-directional domain without assuming a specific spectral shape of the spectrum (Iseki and Ohtsu, 2000; Tannuri et al., 2003). In the context of dynamically positioned ships, records of the wave-induced heave, roll, and pitch motions, assumed to be unaffected by the DP control scheme, can be used for SSE (e.g. Tannuri et al., 2003; Pascoal and Guedes Soares, 2009; Brodtkorb et al., 2018a).

Weaknesses of the use of the WBA in frequency-domain approaches include the dependency on accurate transfer functions (Tannuri et al., 2003). In the context of ship operations (e.g. transportation, docking, lifting, etc.), regularly updated information on the vessel seakeeping model would be an advantage, having in mind that the draught, inertia distribution, and vessel heading, among other operational parameters, can be frequently shifted, which challenges the reliability of precomputed RAOs for online SSE during operations at sea.

Calibration of RAOs refers to a class of system identification techniques to correct available estimates of the RAOs, in order to better describe the linear response behaviour of a ship under prescribed operational and environmental conditions. Some studies were focused on estimating the vessel's hydrodynamic coefficients – i.e. added mass, damping, stiffness, and wave excitation – based on relevant vessel data, wave information, and measurements of the wave-induced responses (Yuan et al., 2016; Kaasen et al., 2020; Skandali et al., 2020). Other research efforts were conducted to tune the important parameters (position of the centre of gravity, mass, transverse metacentric height, additional roll damping, etc.) upon which the hydrodynamic vessel model is determined. In particular, the discrete Bayesian updating formula was exploited in a tuning algorithm with promising results (Han et al., 2021a), although uncertainties from wave information were not considered. Another algorithm, inspired from the scaled unscented Kalman filter, was introduced by Han et al. (2021b) to perform simultaneous tuning of some chosen vessel model parameters and sea state characteristics, based on vessel motion measurements and a parameterized directional wave spectrum. The performance of the method was evaluated through numerical case studies, and it proved to reduce the systematic error and uncertainty of the selected parameters, in both long- and short-crested waves. Finally, an optimization algorithm was presented by Nielsen et al. (2021) for direct tuning of RAOs, using closed-form expressions as initial guess, in addition to vessel response measurements and ERA5 directional wave spectra, with the aim to improve the accuracy of wave-induced response predictions. The optimal tuning parameters were found to minimize the error between the measured response spectrum and the theoretical estimate.

1.1. Content and novelty of study

The topics of sea state estimation and tuning of vessel seakeeping model have historically been treated individually. In fact, those techniques are closely interconnected: on one hand, the correctness of the RAOs with regard to actual conditions is beneficial to the accuracy of sea state estimates when the WBA is employed; on the other hand, calibration procedures for RAOs rely on accurate descriptions of the wave system. One can therefore consider the two-fold problem of simultaneously calibrating, or say, *tuning*, the RAOs of a given vessel (the system) and estimating the sea state (the input to the system, or *source*) when only ship motion measurements (the output, or *observation*) are known. This problem is difficult to solve if a single vessel is considered, because the RAO-tuning (or system identification) method and the SSE (*source estimation*) method are interdependent. Instead, it is herein proposed to solve the problem by considering a network of multiple ships operating at the same time in the same geographical area, i.e. a single-input multi-output (SIMO) system. The idea to consider ships as a *sensor network* for SSE was previously introduced by Nielsen et al. (2019), and the present study constitutes a novel extension of the concept, able to simultaneously: (1) improve the available estimate of the wave-to-motion transfer functions, which was not considered in the original study; (2) and produce an improved estimate of the wave spectrum – in relation to accuracy and precision – when compared to existing WBA methods that neglect any uncertainty in the RAOs. The paper also exhibits further developments in the weighting technique to fuse wave information derived from several vessels. To evaluate the potential of the new concept within the field of marine technology, use is made of a dedicated dataset of model-scale test results for multiple (three) ships in DP in a wave tank, noticing that such a dataset has not before been considered in the related literature.

The proposed procedure uses the main particulars of the ships and the measurements of wave-induced ship motions as the only input, which means that the procedure does not require precomputed vessel RAOs as input. This is seen as a practical advantage in light of possible future implementation in on-board systems for online SSE.

1.2. Composition of paper

The paper is organized as follows. The necessary theoretical background from previous studies on the WBA and tuning of RAOs is summarized in Section 2. Then, the new concepts and methodology for the present study are developed in Section 3. Sections 4 and 5 are focused on two different case studies, one based on numerically simulated data, and the other exploiting data from model-scale experiments. General discussions of the performance of the method are then given in Section 6, and the paper finishes with conclusions and recommendations for future work in Section 7.

2. Theory

2.1. Fundamental assumptions and definitions for the seakeeping analysis

The wave process is assumed to be stationary, ergodic, and Gaussian over the observation time. This enables a linear steady-state approach in the frequency domain. The wave-induced vessel motions can be well estimated by using the linear transfer functions and the wave spectrum.

In line with Brodtkorb et al. (2018a,b), the theory is presented here assuming long-crested waves, which means that the wave system is uniquely described by a 1-D wave spectrum $S_\zeta(\omega)$, where ω is the angular wave frequency. The direction of propagation of the waves μ is defined relative to North, as shown in Fig. 1. The ship heading angle ψ is constant and defined so that $\psi = 0°$ when the ship has the bow towards North. The relative wave direction is defined as $\beta = \mu - \psi$, and it follows that $\beta = 0°$ is a following sea, $\beta = 180°$ is head sea, and $\beta = 90°$ or $270°$ is beam sea.

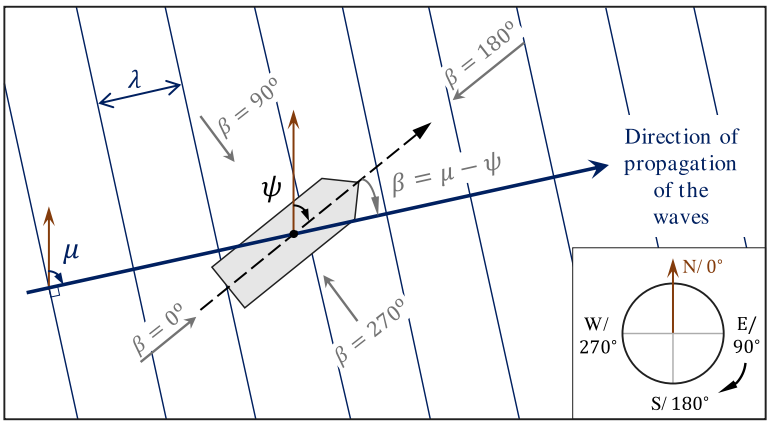

Fig. 1. Definition of the heading angles.

2.2. Shipboard sea state estimation using multiple ships

Let us assume that N ships ($N \geq 2$) are operating in the same time frame in the same open-water geographical area. The ships are far enough apart to avoid ship-to-ship interactions from radiated and diffracted waves, but close enough to experience the same sea conditions. By inspecting re-analysis wave data interpolated along many ship route paths, two studies (Nielsen, 2021; Nielsen and Ikonomakis, 2021) revealed a substantial level of spatial variation, for frozen time, in the sea state parameters, like significant wave height, zero-crossing period, and mean wave direction. This variability – added up with the temporal evolution of sea state characteristics – challenges the commonplace assumption of a stationary seaway in periods of up to three hours, which is likely violated for ships sailing at the typical service speed (15–20+ knots). Therefore, it is not trivial to quantitatively set lower and upper bounds for the characteristic distance separating the ships during the observation, and herein it is assumed such limits may be affected by operational factors (e.g. the advance speed) and environmental conditions (e.g. the severity and changeability of the sea state). This question should be tackled in future studies. In practical situations such as ships sailing along the same route path, the number of ships N to be included in the proposed procedure will also depend on the allowable limits for the distance by which they are separated apart. For the present study, let us assume that a characteristic distance of a few kilometres between the stationary ships (2–20 km apart) enables to consider that the N ships experience the same original wave system, undisturbed by interaction with other ships.

The theoretical foundations for sea state estimation using multiple ships were laid in Nielsen et al. (2019). The WBA was used in a network of ships sailing at the same time in the same geographical area. The study introduced fundamental concepts for data fusion, especially the weighting of ship-specific wave spectrum estimates, and proposed an uncertainty measure of the so-called weighted wave spectrum.

2.2.1. Weighting of the ship-specific wave spectrum estimates

Let us consider the response R of a given ship $n \in \{1...N\}$, for example, the motion in one of the six rigid-body degrees of freedom (DoF). Throughout our study with multiple ships, the transfer function of ship n for this response is denoted $\Phi_R^{(n)}(\omega;\beta)$.

A major advantage in considering a network of ships for SSE is that the sea state observations derived via measurements collected from several vessels offer the possibility to compute an – expectedly more accurate – weighted sea state estimate. The weights attributed to the individual wave spectrum estimate from each ship are frequency-dependent. They are calculated in three steps and are based on the moduli of the transfer functions for a selected response R. First, Eq. (1) computes a mean RAO $\bar{\Phi}_R^{(n)}(\omega)$, by averaging the moduli $|\Phi_R^{(n)}(\omega;\beta)|$ of the transfer functions with respect to wave heading β:

$$\bar{\Phi}_R^{(n)}(\omega) \equiv \underset{\text{All } \beta}{\text{mean}} \left[|\Phi_R^{(n)}(\omega;\beta)| \right], \quad n = 1...N \tag{1}$$

This enables to avoid the dependency in the wave direction in the spectrum weightings.

Secondly, the (frequency-dependent) mean modulus obtained from Eq. (1) is normalized by its maximum value with respect to wave frequency — emphasizing here that the maximum value is ship-specific. This is performed for a single ship n in Eq. (2):

$$\sigma_R^{(n)}(\omega) \equiv \frac{\bar{\Phi}_R^{(n)}(\omega)}{\max_\omega \bar{\Phi}_R^{(n)}(\omega)}, \quad n = 1...N \tag{2}$$

Once the normalized modulus $\sigma_R^{(n)}(\omega)$ is calculated, the frequency-dependent weights $\rho_R^{(n)}(\omega)$ are computed as the ratio of the considered ship's normalized modulus $\sigma_R^{(n)}(\omega)$ and the sum of the normalized moduli $\sigma_R^{(p)}(\omega)$ over all ships $p = 1...N$, see Eq. (3):

$$\rho_R^{(n)}(\omega) \equiv \frac{\sigma_R^{(n)}(\omega)}{\sum_{p=1}^{N} \sigma_R^{(p)}(\omega)}, \quad n = 1...N \tag{3}$$

This definition ensures that the weights have a lower bound of 0, a higher bound of 1, and that the sum of the ship-specific weights equals 1 at any frequency.

A sensitivity study of the response considered for the weighting process was made by Nielsen et al. (2019), and in particular heave-based $\rho_z^{(n)}(\omega)$ and pitch-based $\rho_\theta^{(n)}(\omega)$ weightings were shown to perform well for SSE. The present study considers both types of weighting but introduces as well the combination of heave-based and pitch-based, that is $R = \{z, \theta\}$, considering their geometric and arithmetic means as two alternative weightings $\rho_{\text{arithm}}^{(n)}(\omega)$ and $\rho_{\text{geom}}^{(n)}(\omega)$, respectively; these are defined in Eqs. (4) and (5):

$$\begin{aligned} \rho_{\text{arithm}}^{(n)}(\omega) &\equiv \frac{\frac{1}{2}\left(\sigma_z^{(n)}(\omega) + \sigma_\theta^{(n)}(\omega)\right)}{\sum_{p=1}^{N} \frac{1}{2}\left(\sigma_z^{(p)}(\omega) + \sigma_\theta^{(p)}(\omega)\right)} \\ &= \frac{\sigma_z^{(n)}(\omega) + \sigma_\theta^{(n)}(\omega)}{\sum_{p=1}^{N}\left(\sigma_z^{(p)}(\omega) + \sigma_\theta^{(p)}(\omega)\right)}, \quad n = 1...N \end{aligned} \tag{4}$$

$$\rho_{\text{geom}}^{(n)}(\omega) \equiv \frac{\sqrt{\sigma_z^{(n)}(\omega) \cdot \sigma_\theta^{(n)}(\omega)}}{\sum_{p=1}^{N} \sqrt{\sigma_z^{(p)}(\omega) \cdot \sigma_\theta^{(p)}(\omega)}}, \quad n = 1...N \tag{5}$$

where $\sigma_z^{(n)}(\omega)$ and $\sigma_\theta^{(n)}(\omega)$ are the heave-based and pitch-based normalized moduli for ship n, respectively.

Irrespective of the considered weighting type, the weighted wave spectrum $\overline{\hat{S}_\zeta}(\omega)$ is finally obtained according to Eq. (6):

$$\overline{\hat{S}_\zeta}(\omega) = \sum_{n=1}^{N} \rho^{(n)}(\omega) \cdot \hat{S}_\zeta^{(n)}(\omega) \tag{6}$$

where $\hat{S}_\zeta^{(n)}(\omega)$ is the ship-specific wave spectrum estimate from ship n, and $\rho^{(n)}(\omega)$ is the weighting computed by the arithmetic mean, Eq. (4), or geometric mean, Eq. (5).

To sum up, at a given frequency, higher weight is assigned to a ship that has a larger response amplitude operator for the given frequency. As an effect of wave filtering, the signal-to-noise ratio is worsened at frequencies where there is a low response amplitude, which is a source of uncertainty in the corresponding wave estimate. The weighting favours the portions of each individual estimate that have suffered the least wave filtering in relation to the other ships' responses. The error of the resulting weighted spectrum is considerably reduced compared to a baseline case where all individual spectra would be given equal weight at all frequencies, as was shown in Nielsen et al. (2019).

2.2.2. Uncertainty measure of wave spectrum estimate

A measure of the uncertainty of the weighted wave spectrum estimate $\overline{\hat{S}_\zeta}(\omega)$ from Eq. (6) was proposed in Nielsen et al. (2019). It is based on the discrepancy between the individual ship-specific spectrum estimates $\hat{S}_\zeta^{(n)}(\omega)$.

The frequency-dependent uncertainty measure $\Delta(\omega)$ is defined by:

$$|\Delta(\omega)|^2 \equiv \sum_{n=1}^{N-1} \sum_{l=n+1}^{N} \left[|\hat{S}_\zeta^{(n)}(\omega) - \hat{S}_\zeta^{(l)}(\omega)|^2 \right] \tag{7}$$

where, at a given frequency, larger deviations between the spectral densities express larger uncertainty at the given frequency.

The total uncertainty Ψ is calculated in an integrated form considering the whole range of frequencies:

$$\Psi \equiv \frac{\frac{1}{N}\int_0^\infty \Delta(\omega) d\omega}{\int_0^\infty \overline{\hat{S}_\zeta}(\omega) d\omega} \tag{8}$$

The defined uncertainty measure should be regarded as a measure of the variance, or precision, among individual sea state estimates coming from different observation platforms. It is important to note that it does not reveal anything about the bias error with respect to the (true) encountered sea state. Nonetheless, the weighting's purpose is that, if many individual sea state estimates can be collected from independent measurements on board different observation platforms, then the bias error of the weighted estimate should tend to zero.

2.2.3. Error measure of wave spectrum estimate

To quantify the level of error $\bar{e}$ in the sea state estimates, a difference metric between the (true) generating wave spectrum $S_\zeta(\omega)$ and an estimate $\hat{S}_\zeta(\omega)$ can be defined as the normalized "area-deficit" encased by the two spectra:

$$\bar{e} \equiv \frac{\int_0^\infty |S_\zeta(\omega) - \hat{S}_\zeta(\omega)| d\omega}{\int_0^\infty S_\zeta(\omega) d\omega} \tag{9}$$

The computation of this metric is only possible if simulated data is considered, that is when the true wave spectrum is known.

2.3. Tuning of transfer functions

Applying a discrete Fourier transform to the time series of a measured response yields a measured response auto-spectrum $\tilde{S}_{RR}(\omega)$, where the tilde indicates that the data is of experimental nature. Note that, in light of the case studies focused on DP-operated ships, zero-forward speed is assumed here for the ships.

On the other hand, a response spectrum $\hat{S}_{RR}(\omega)$ can be estimated theoretically through the relationship given in Eq. (10):

$$\hat{S}_{RR}(\omega) = |\hat{\Phi}_R(\omega;\beta)|^2 \cdot E(\omega) \tag{10}$$

where $\hat{\Phi}_R(\omega;\beta)$ is the estimated transfer function and $E(\omega)$ is a generic notation for the 1-D wave spectrum.

Because of the uncertainty in operational parameters and the possible violation of the fundamental assumptions (linearity, stationary conditions) for the seakeeping model, it is proposed in Nielsen et al. (2021) to write a better estimate of the transfer function $\hat{\Phi}_R(\omega;\beta)$ as in Eq. (11):

$$\hat{\Phi}_R(\omega;\beta) = \hat{\Phi}_{R,0}(\omega;\beta)(1 + \alpha_R(\omega)) \tag{11}$$

where $\hat{\Phi}_{R,0}(\omega;\beta)$ is the initial estimate and $\alpha_R(\omega)$ is a tuning coefficient, which depends on the wave frequency. The tuning coefficients for the same response R can be grouped into a vector $\boldsymbol{\alpha}_R = [\alpha_R(\omega_1), \alpha_R(\omega_2), \ldots, \alpha_R(\omega_K)]$ of tuning coefficients associated with the discretized range of frequencies $[\omega_1, \omega_2, \ldots, \omega_K]$. This vector is returned from an optimization procedure to minimize – in the least squares sense – the gap between the measured and theoretical response spectra, i.e $\tilde{S}_{RR}(\omega)$ and $\hat{S}_{RR}(\omega)$, respectively. The corresponding cost function to be minimized is given in Eq. (12):

$$\begin{aligned} f_R(\boldsymbol{\alpha}_R) &\equiv \sum_{k=1}^{K} \left| \tilde{S}_{RR}(\omega_k) - \hat{S}_{RR}(\omega_k) \right|^2 \\ &= \sum_{k=1}^{K} \left| \tilde{S}_{RR}(\omega_k) - |\hat{\Phi}_R(\omega_k;\beta)|^2 E(\omega_k) \right|^2 \\ &= \sum_{k=1}^{K} \left| \tilde{S}_{RR}(\omega_k) - |\hat{\Phi}_{R,0}(\omega_k;\beta)(1+\alpha_R(\omega_k))|^2 E(\omega_k) \right|^2 \end{aligned} \tag{12}$$

where $\boldsymbol{\alpha}_R$ is the optimization variable, which enters the right-hand side of Eq. (12) through $\hat{\Phi}_R$.

Note that this is a simplified expression for the cost function, compared to the one given in Nielsen et al. (2021), which deals with non-zero forward speed problems in short-crested waves.

3. Methodology

The core of the method for sea state estimation using a network of ships, through simultaneous SSE and tuning of RAOs, is now presented in detail.

3.1. General overview of the main algorithm

Algorithm 1, given in a pseudo-code format in Appendix A, describes the iteration process in the general case with N ships. The present paper does not deal with the topology of the network (Yu et al., 2022), which will be studied in future work. It is herein assumed that an all-to-all interconnection scheme is in place, meaning that each ship is directly connected to all the other ships.

3.2. Initialization of the wave-to-motion transfer functions by closed-form expressions

It is considered that the response R is sampled and recorded by shipborne sensors, e.g. an inertial motion unit (IMU). For a given ship n, we denote $\mathcal{R}^{(n)}$ as the set of vessel responses for which data is accessible.

This study makes use of inexpensive transfer functions calculated by closed-form expressions (CFEs) developed by Jensen et al. (2004) for a box-shaped ship. Such an approach is practical if detailed information about the hull geometry is not available, or if the (higher-fidelity) transfer functions simply are missing. The required input information for the procedure is limited to the main dimensions — namely the length L, breadth B, draught T, and block coefficient C_B, together with the advance speed and heading. One can reasonably assume that this basic information is immediately available to most ship operators. The CFEs are evaluated in a fraction of a second, but the fidelity of such

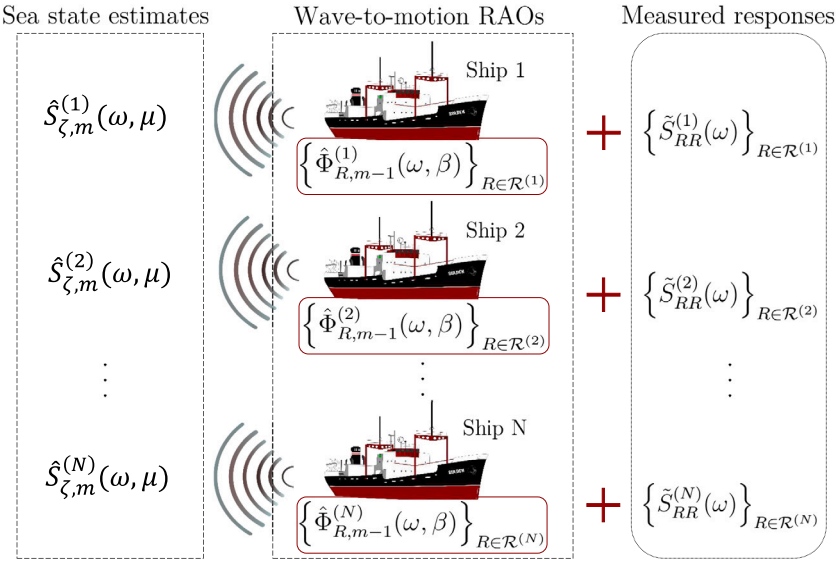

Fig. 2. Illustration of the sea state estimation step in one iteration of the main algorithm.

a model may be compromised, as the shape of the hull is simplified. In the implementation, the CFE will be used to calculate initial values before carrying out an iterative approach where the transfer functions are tuned. The initial estimate of the transfer function for the response R of ship n is denoted $\hat{\Phi}^{(n)}_{R,0}$. Note that the $(\omega;\beta)$ indexing will be avoided in the remaining of the paper, to ease readability.

3.3. The iterative process: simultaneous SSE and RAO-tuning

In each iteration $m \geq 0$ of the algorithm two main tasks are performed: the SSE step and the RAO-tuning step.

3.3.1. Implementation of the SSE step

The concept for this step is illustrated in Fig. 2. For each vessel $n = 1...N$, an estimate of the wave spectrum is computed, employing the WBA, using: (1) the available measured response spectra $\left\{\tilde{S}^{(n)}_{RR}(\omega)\right\}_{R\in\mathcal{R}^{(n)}}$ for several responses; (2) and the estimates $\left\{\hat{\Phi}^{(n)}_{R,m-1}\right\}_{R\in\mathcal{R}^{(n)}}$ of the associated transfer functions available from the previous iteration $m-1$. The SSE step returns N distinct sea state estimates, $\left\{\hat{S}^{(n)}_{\zeta,m}\right\}_{n=1...N}$, discretized in the 2-D space (ω_j, β_k).

In principle, the ships could use different methods for obtaining an estimate of the 1-D wave spectrum. In this paper, a nonparametric method, developed earlier by Brodtkorb et al. (2018a,b) for applications related to DP, was chosen for all ships. Its main feature is an iterative procedure to match the spectral energy distribution between the measured response and theoretical calculations based on RAOs. The method is very efficient in its computations, due to the fundamental assumptions upon which it is built, as explained below.

The original SSE algorithm assumes long-crested waves and was invented for ships in stationkeeping, equipped with a dynamic positioning system, meaning that zero-forward speed is assumed. It also enables the estimation of the incoming wave direction. However, in the present study, the relative wave direction β is given as input, simplifying the sea state estimation procedure, and hence only two symmetric responses, namely heave z and pitch θ, are considered. The roll response is disregarded because there is no need to distinguish between port and starboard incident waves.

The gains in the iteration scheme are chosen to satisfy the stability criterion given in Brodtkorb et al. (2018b) with a conservative margin (i.e. low gains); indeed, it was observed that low values for the gains benefit the convergence of the main algorithm. The maximum number of iterations per response was set to 50 in Case study 1 and 25 in Case study 2. Those values were found to yield the best estimation performance on the selected ships and sea states. The SSE loop is repeated independently for each pair of responses and each ship. The reader is referred to the cited original studies for further details.

3.3.2. Implementation of the RAO-tuning step

The concept for this step is illustrated in Fig. 3. For one specific vessel n, with $n \in \{1...N\}$, the RAO estimates are improved through tuning. To perform this tuning task, three inputs are needed for each response R: (1) the initial guess of the RAOs $\hat{\boldsymbol{\Phi}}^{(n)}_{R,0}$ (in our case, the CFE), (2) the measured response spectrum $\tilde{S}^{(n)}_{RR}$, and (3) an estimate of the wave spectrum. Concerning the latter, the input is obtained by data fusion, applying a ship-specific weighting to the N individual wave spectrum estimates obtained from the SSE step. The weighting function is computed from the RAOs, as per Eqs. (1) to (6). It is noticed that the individual sea state estimate $\hat{S}^{(n)}_{\zeta,m}$ produced by ship n is not independent of the corresponding ship RAOs and measured response spectra. Thus, it is thought that $\hat{S}^{(n)}_{\zeta,m}$ should not be used to tune the RAOs of ship n, to avoid the propagation of errors within the model. In the so-called *leave-one-out weighting* process, zero weight is given at all frequencies to the individual wave spectrum estimate produced by the ship that is being tuned. The weighted wave spectrum used to tune the RAOs of ship n is denoted $\overline{\hat{S}}^{(n)}_{\zeta,m}$. The RAO-tuning step is repeated for each ship, that is $n = 1...N$, and a new estimate of the RAOs is produced for each, that is the set of functions $\left\{\left\{\hat{\boldsymbol{\Phi}}^{(n)}_{R,m}\right\}_{R\in\mathcal{R}^{(n)}}\right\}_{n=1...N}$ is eventually obtained.

As stated in Section 2.3, an optimization problem must be solved to minimize the cost function of Eq. (12). Contrary to what was done in Nielsen et al. (2021), bound constraints are imposed on the tuning coefficients: α_R is allowed to be in the range $[-0.2, 0.2]$, thus ensuring that the original closed-form RAOs are not too distorted after tuning. This constraint is observed to be necessary; otherwise, the sea state estimates computed via the tuned RAOs become unrealistic themselves, causing a risk to the stability of the algorithm. This is further discussed in Section 6.

The Trust-Region Constrained algorithm developed by Byrd et al. (1999) is exploited to solve the optimization problem, noticing that implementation in Python 3 is available in the optimization library

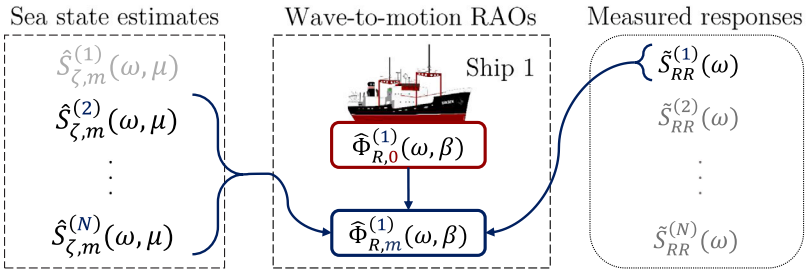

Fig. 3. Illustration of the RAO-tuning step in one iteration of the main algorithm. For clarity, the process is represented for ship number 1 only.

Table 1
Main particulars of the three considered ships for Case study 1.

	RV	PSV	FPSO	
Length between perpendiculars, L_{pp}	28.9	82.8	200.0	[m]
Breadth middle, B	9.6	19.2	44.0	[m]
Draught, T	2.63	6.00	12.00	[m]
Displacement, Δ	418.06	6362.21	100409.92	[t]
Block coefficient, C_B	0.559	0.651	0.928	[-]

Table 2
Scenarios of simulation for Case study 1, in terms of the relative wave heading and generating sea state at the vessel's point of operation. The vessels have zero forward speed.

Scenario nr.	Sea state parameters			RV	PSV	FPSO
	H_s [m]	T_p [s]	γ [-]	β [°]	β [°]	β [°]
A	2.0	8.0	3.3	130	160	100
B	2.0	10.0	1	130	160	100
C	2.0	12.0	1	130	160	100

of SciPy, under the function `minimize` with the method `'trust-constr'`.[1] This optimization algorithm was chosen because it enabled fast convergence in most of the tested cases. Quasi-Newton methods (among others, BFGS) were also tried without the bound constraints, but they did not feature as good convergence performances as the Trust-Region Constrained algorithm.

4. Case study 1: Numerical simulation with three ships

4.1. Scope

A simulation study is performed with three vessels: the NTNU-owned research vessel Gunnerus (denoted "RV"), a platform supply vessel ("PSV"), and a Floating Production Ship Offloading ("FPSO"). Their main particulars are given in Table 1. Considering the WBA framework, the vessels will behave as low-pass filters with respect to the waves, with different cut-off frequencies since they have different dimensions.

The responses are simulated in the frequency domain. For this purpose, different sea states are defined. In total, three scenarios are examined, with significant wave height H_s, peak period T_p, peak shape parameter γ, and relative wave headings β given in Table 2. The corresponding wave spectra are plotted in Fig. 4, noticing that the (generalized) JONSWAP spectrum (Hasselmann et al., 1973) is assumed in all cases. The value of the significant wave height is unimportant, since the linear ship motions are directly proportional to H_s, emphasizing that normalized error metrics are used in the results sections. The relative wave headings are also arbitrarily chosen and different for the three vessels, see Table 2, corresponding to head sea, bow sea and beam sea conditions for PSV, RV and FPSO, respectively. In the context of offshore operations, three parallel vessels would be a more specific configuration, which is briefly considered later in Section 6. The headings remain unchanged during the three scenarios, to focus the sensitivity study on the environmental parameters. Notably, three different peak wave periods are tried, to vary the excitation within the frequency range of ship motions. With the chosen γ, scenario A models a unimodal, developing sea state in a fetch-limited situation, typical of strong wind conditions in a relatively restricted water body. Besides, scenarios B and C model a fully-developed sea state in the ocean.

[1] The default values in the Python function were used for the tolerances for termination, while the maximum number of algorithm iterations was set to 1500 (the default was 1000).

Realism of the study is introduced by working with a set of theoretical RAOs purely used for generating the wave-induced responses. To serve this purpose, "ground-true" heave and pitch RAOs of the vessels were obtained from the commercial hydrodynamic codes ShipX and WAMIT. The RAOs are plotted in Fig. 5 for several relative wave headings, and compared with the closed-form expressions (CFE) (Jensen et al., 2004) that the study uses in the SSE and tuning algorithms. It seems important to underline that there is a clear bias in the initial CFE estimate, compared to the true RAOs. The CFE almost always underestimate the RAOs, in such a way that the drop in heave and pitch amplitudes appears at lower frequencies than for the ShipX/WAMIT RAOs. This questions the validity of the assumption followed in the theoretical formulation of the RAO-tuning method, according to which the error between the initial estimate and the true RAO is normally distributed; cf. the imposed bounds for the tuning coefficients, as indicated in Section 3.3.2. It is admitted that this bias may have negative consequences on the performance of both the RAO-tuning and SSE steps. As a general recommendation, one should always try to use unbiased RAOs for SSE. However, it is understood that the aim of the tuning step is mainly to reduce such bias, which motivates the use of the CFE to test (and challenge!) the overall architecture. The use of other sets of – perhaps less biased – RAO estimates is discussed in Section 6.

4.2. Results and discussions

4.2.1. Comparison of the weighting functions

The four types of weighting introduced in Section 2.2.1 are represented for the three ships in Fig. 6, corresponding to the first iteration. Those weights do not vary significantly over iterations. Note that this observation is not correlated to the performance of the algorithm, nor does it reveal any indication of the amount of tuning that the RAOs undergo, but instead, it is an expected result from the definition of the weighting functions, cf. Eqs. (1) to (3). In fact, in long-crested waves, the tuning concerns only one direction, namely the observed heading β, which means that only one column of the original RAO matrix $\hat{\boldsymbol{\Phi}}_{R,0}^{(n)}$ is altered after tuning. On the other hand, the calculation of the weighting function involves the whole set of RAOs, considering all possible headings $[0°, 10°, \dots, 350°]$ – or, equivalently, all columns of $\hat{\boldsymbol{\Phi}}_{R,0}^{(n)}$ –, of which 35 (out of 36) have not undergone tuning, since they did not correspond to the observed heading. Thus, the effect of tuning the RAOs is almost imperceptible when evaluating the weights iteration

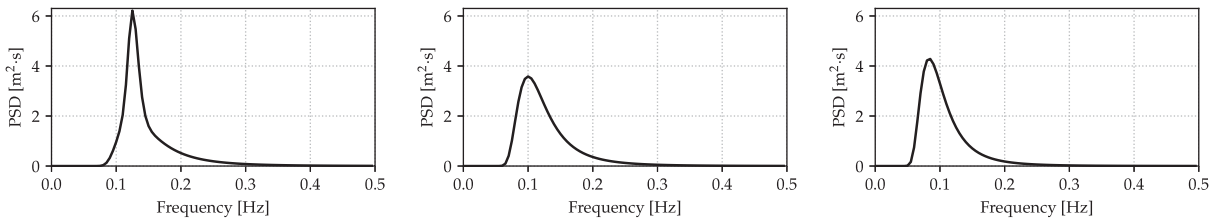

(a) $H_s = 2.0$ m, $T_p = 8.0$ s, $\gamma = 3.3$ (b) $H_s = 2.0$ m, $T_p = 10.0$ s, $\gamma = 1$ (c) $H_s = 2.0$ m, $T_p = 12.0$ s, $\gamma = 1$

Fig. 4. 1-D wave spectra for sea states 1 to 3 in Case study 1. PSD stands for power spectral density.

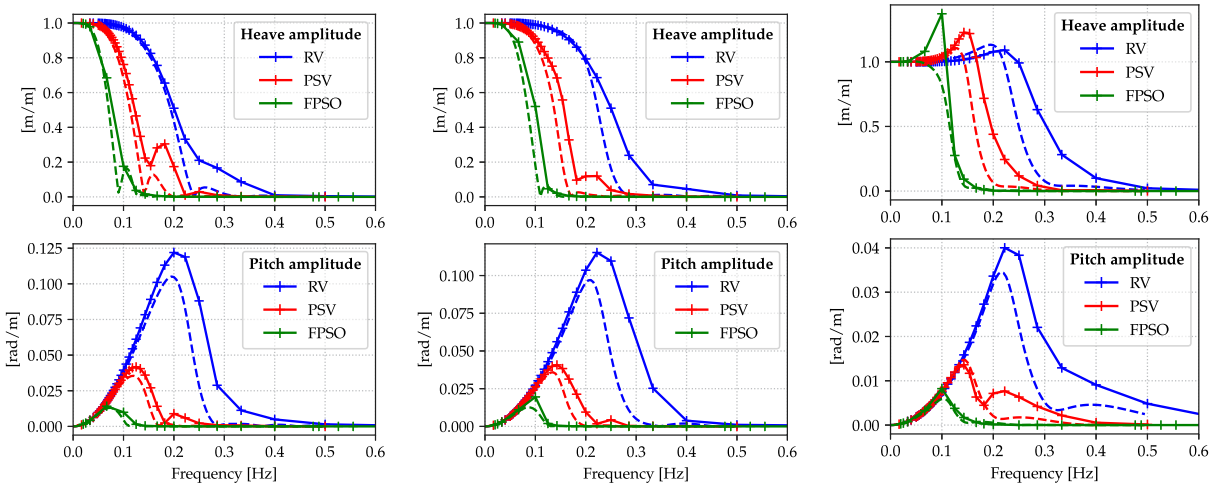

(a) $U = 0$ m/s, $\beta = 160°$ (b) $U = 0$ m/s, $\beta = 130°$ (c) $U = 0$ m/s, $\beta = 100°$

Fig. 5. Heave and pitch RAOs of the three ships selected for Case study 1. The solid lines represent theoretical RAOs obtained from strip theory (ShipX, for RV and PSV) or a potential flow solver (WAMIT, for FPSO), while the dashed lines correspond to the closed-form expressions given in Jensen et al. (2004). Note the different vertical scales in the subplots.

after iteration.[2] What is more, in scenarios of short-crested waves, left for future work, it suffices to say that the tuning will concern a larger set of headings due to the wave spreading, resulting in more columns of the original RAO matrix $\hat{\boldsymbol{\Phi}}_{R,0}^{(n)}$ to be altered. Consequently, the weights would be seen to vary more significantly over iterations.

In the present study, the weighting using the arithmetic mean was preferred, because (1) it does not give more importance to heave or pitch, and (2) the ships have almost equal contributions at very low frequencies, which supports the idea that the ships all behave as low-pass filters. At frequencies over 0.1 Hz, arithmetic and geometric mean are essentially the same. In particular, RV's estimates are given high importance, while the FPSO's contribution is nearly zero.

4.2.2. Effects of the RAO-tuning step after one iteration of the main algorithm

To visualize the effect of tuning the RAOs, it is interesting to compare the ship-specific wave spectrum estimates before and after the tuning step is performed. This is shown in Fig. 7 for scenario C, and additional results are given in Appendix B for the other two scenarios. Overall, it is seen that the individual wave spectra from the three ships after RAO-tuning show a better agreement with one another and with the true generating spectrum, compared to the first sea state estimates using the original (not-tuned) closed-form RAOs. From this figure, it can be interpreted that the uncertainty with which the sea state is estimated is decreased thanks to the tuning step; indeed, there is a reduced discrepancy, i.e. variance, in the set of wave spectrum estimates when evaluated frequency by frequency.

The weighted wave spectra from the ships are shown in Fig. 8 for the three scenarios, before and after tuning of the RAOs, denoted "CFE" and "Tuned CFE" respectively in the figure, and compared with the generating JONSWAP spectrum. It is observed that the weighted estimate after the RAO-tuning step is in general better. In particular for scenarios A and C, the energy density at the peak is more accurately estimated, compared to the estimate without any tuning. For scenario B, there is only a very slight improvement of the weighted spectrum estimate over the whole range of wave frequencies, although the individual estimates are significantly improved after tuning (see Fig. B.24).

The transfer functions and tuning coefficients used to obtain the estimates in Fig. 8-(c), i.e. for scenario C, are plotted in Figs. 9 and 10, respectively. It is seen that some of the RAOs, especially for RV (in heave and pitch), become quite non-physical after tuning. This might be an issue if the tuned RAOs were used a posteriori for other purposes than SSE, but this is out of the scope of the present study and is already discussed by Nielsen et al. (2021). It is remarkable that the tuning step makes efforts to correct the CFE, but such corrections do not necessarily result in a better match with the true RAOs. For FPSO in heave, and PSV in pitch, the agreement is better, however, for RV in heave, the tuned RAO underpredicts amplitude at frequencies under 0.17 Hz. One reason why the tuned RAO estimates are worse for RV could be that the "leave-one-out" tuning method for this vessel makes use of the wave spectrum estimates from PSV and FPSO only, which are not as good as those from RV, as seen in Fig. 7-(a). Indeed, the initial sea state estimates from PSV and FPSO significantly overpredict the energy

[2] Alternatively, a heading-dependent weighting function could be introduced, as discussed in Nielsen et al. (2019), but such a function would then evolve notably after iterations, which might be a concern for the convergence of the algorithm.

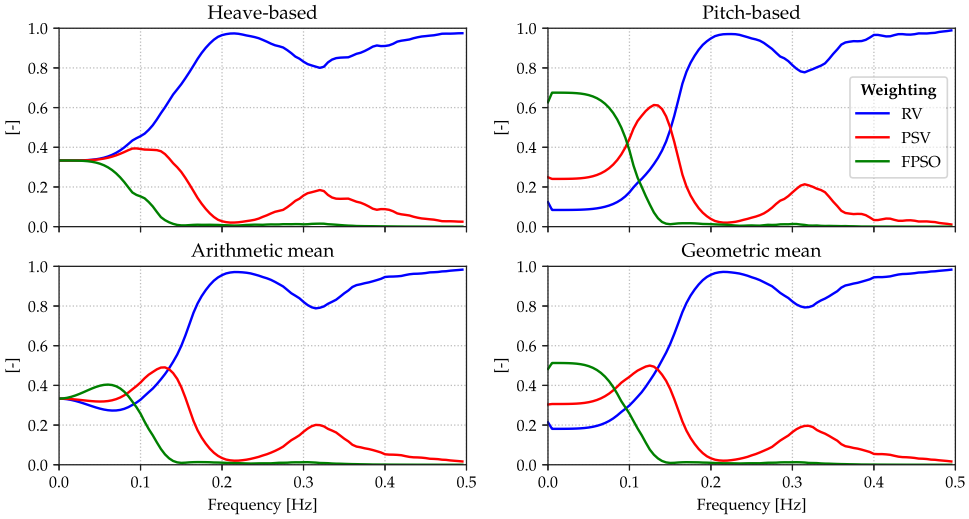

Fig. 6. Ship-specific weighting functions in Case study 1. These are derived from the moduli of different transfer functions. Top left: heave-based weighting; Top right: pitch-based weighting; Bottom left: arithmetic mean of heave and pitch-based weightings (chosen for Case study 1); Bottom right: geometric mean of heave and pitch-based weightings.

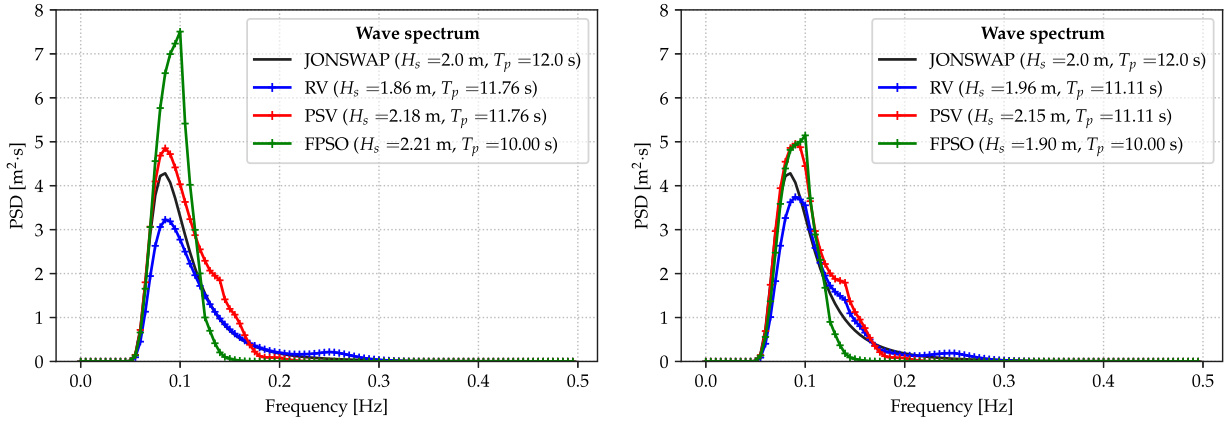

(a) Using *original* closed-form RAOs (b) Using *tuned* closed-form RAOs

Fig. 7. Exact and estimated wave spectra from the three ships selected for scenario C of Case study 1. Left: estimates before any tuning of the RAOs, that is using the original closed-form expression; Right: estimates using the tuned RAOs.

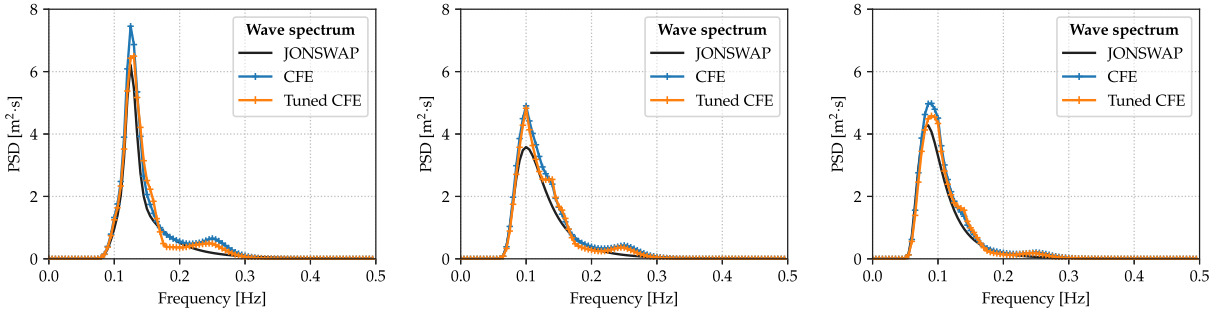

(a) Scenario A (b) Scenario B (c) Scenario C

Fig. 8. Weighted wave spectra in the three scenarios of Case study 1. The solid lines represent the generating wave spectra, while the lines with plus markers correspond to estimates in the WBA framework. "CFE" refers to the estimate before tuning the RAOs, that is using the original closed-form expression, while "Tuned CFE" uses the tuned RAOs.

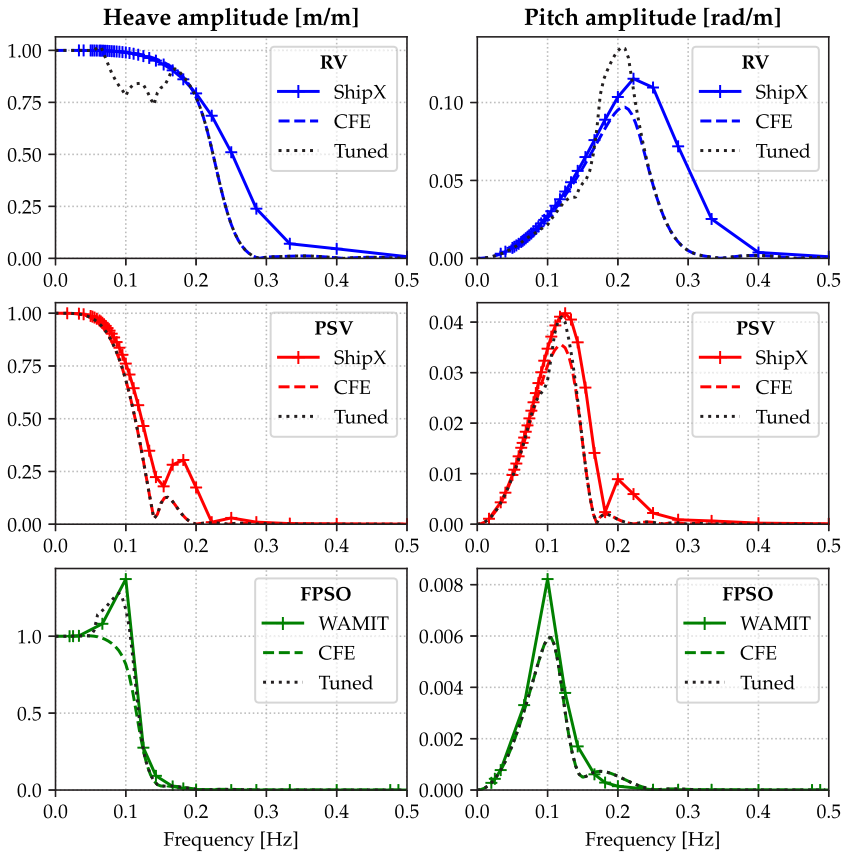

Fig. 9. Heave and pitch RAOs of the three ships selected for scenario C of Case study 1. The lines with plus markers represent the theoretical RAOs, the dashed lines correspond to the closed-form expressions (CFE) given in Jensen et al. (2004), and the black dotted lines are the tuned RAOs obtained at the end of the first iteration. Note the superimposition of the two latter in the case of PSV for heave and FPSO for pitch.

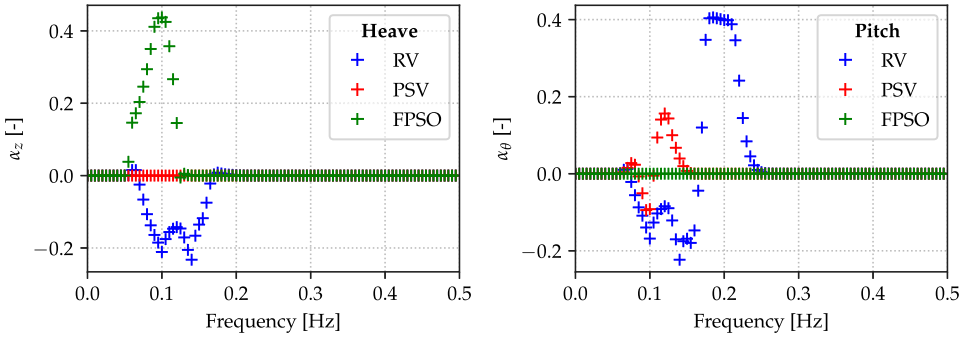

Fig. 10. Tuning coefficients for the heave and pitch RAOs of the three ships selected for scenario C of Case study 1.

density around the peak. From that, it can be inferred that there is a trend for a somewhat symmetrical behaviour between the SSE and RAO-tuning steps, meaning that overprediction in a frequency range within one step is likely to result in an underprediction at the same frequencies at the other step, and vice-versa.

Since the ship headings do not vary with scenario number, the tuned RAOs for scenarios A and B are very similar to those from scenario C, see Fig. 9, and the comments from the last paragraph apply to them too.

4.2.3. Convergence study of the main algorithm

On average, it takes approximately 60 s to run one iteration of Algorithm 1 on the available laptop (CPU Intel(R) Core(TM) i7-10510U CPU @ 1.80 GHz, 16 GB memory). Since the computations are relatively fast, it is possible to investigate what happens for the sea state estimates after running more iterations of Algorithm 1. In particular, the SSE results are analysed in terms of their precision and accuracy.

As a reminder, the integral-form uncertainty measure is defined in Eq. (8) as the integral of the frequency-dependent variation among ship-specific spectrum estimates, normalized by the variance of the wave process. The evolution of this uncertainty measure versus the number of iterations (ten in total) is shown in Fig. 11 for the three scenarios. It is seen that the sea state estimates become significantly more precise after the first iteration. The uncertainty converges towards an asymptotic value for scenarios A and B, while it is oscillating for scenario C. A clear explanation could not be found for why a scenario leads to a more oscillatory behaviour than the others. Overall, it can be argued that just one iteration can be sufficient to reduce the uncertainty of the sea state estimates.

The error of the weighted wave spectrum relative to the generating wave spectrum is also computed, according to its definition in Eq. (9).

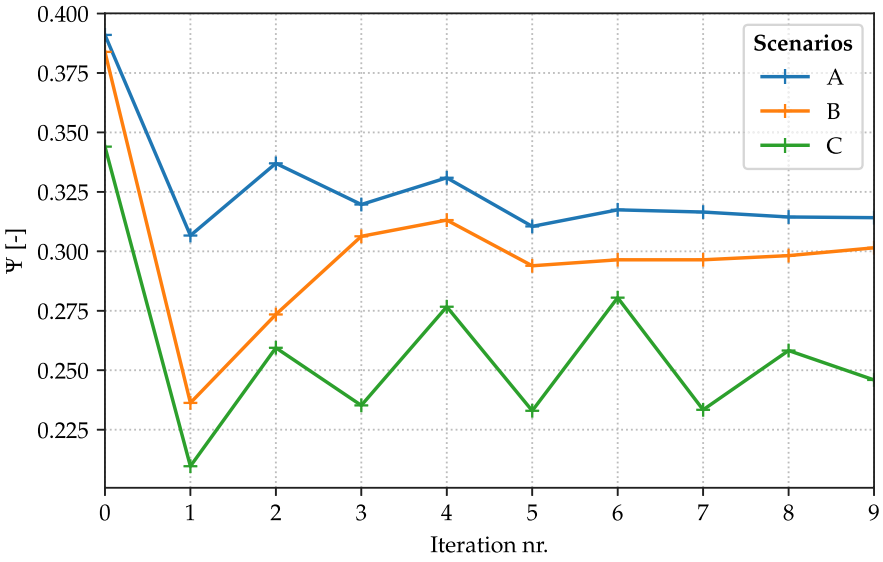

Fig. 11. Uncertainty measure versus number of iterations, for the three scenarios of Case study 1.

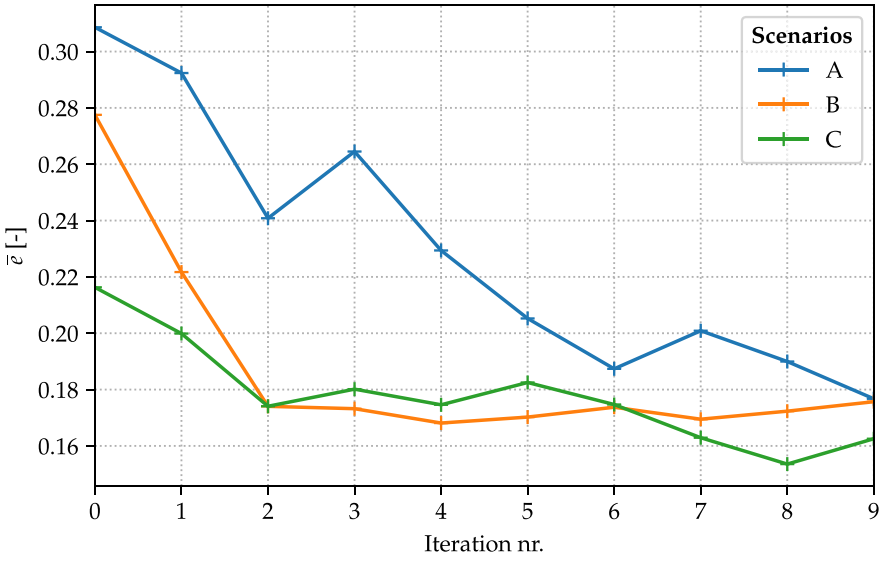

Fig. 12. Normalized error of the sea state estimate versus number of iterations, for the three scenarios of Case study 1.

It is plotted against the number of iterations in Fig. 12. The normalized error decreases until it reaches a (quite) stable value. The convergence is slower for scenario A.

The main results from Case study 1 are gathered in Table 3, in terms of estimated sea state parameters, normalized error and integral-form uncertainty, all obtained at the end of iterations 0, 1, and 4. It is emphasized that H_s, T_p and $\bar{e}$ values are derived from the weighted wave spectrum estimates at successive iterations. Iteration 0 makes use of the original CFE, iteration 1 utilizes the tuned CFE, and, at iteration 4, the RAOs have been tuned four times. From this outcome, it is clear that in all three considered scenarios, the proposed procedure succeeds to provide both more accurate and less uncertain estimates of the sea state. If the SSE results are regarded as a set of ship-specific individual estimates, it seems that the uncertainty evaluated from this set is minimal after just one iteration of the main algorithm, that is after tuning the CFE only once. This finding is further discussed in Section 6.

5. Case study 2: Application of the method to model-scale data

In this section, Algorithm 1 is tested on experimental model-scale data, obtained from CH-TPN Wave Tank, São Paulo, Brazil, in 2019.

Table 3
Results from Case study 1, at the end of iterations 0, 1, and 4.

Scenario	H_s [m]			T_p [s]			$\bar{e}$ [-]			Ψ [-]		
	0	1	4	0	1	4	0	1	4	0	1	4
A	2.26	2.17	2.15	8.0	7.7	8.0	0.309	0.292	0.229	0.391	0.307	0.331
B	2.24	2.14	2.04	10.0	10.0	10.0	0.278	0.222	0.168	0.384	0.236	0.313
C	2.18	2.11	2.04	11.1	11.1	11.1	0.216	0.200	0.175	0.344	0.210	0.277

5.1. Presentation of the experimental set-up and tested scenarios

Three model-scale ships, namely “M510A”, “M510B”, and “PSVH”, with dimensions given in Table 4, have been placed with zero forward speed in a square wave tank and aligned differently so that different wave headings were experienced. The vessel motion responses were recorded for two different long-crested sea states, both of them using a JONSWAP spectrum to model a developing sea. The corresponding scenarios are described in Table 5, in terms of wave spectral parameters and relative wave headings. A photograph and a diagram of the experimental set-up are given in Figs. 13 and 14, where the placement

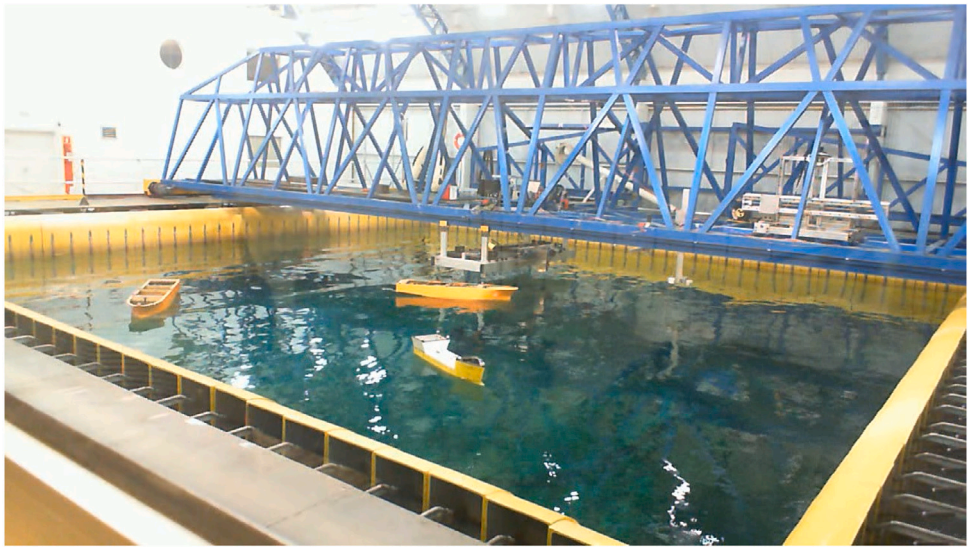

Fig. 13. Picture of the experimental set-up at the CH-TPN Wave Tank facility.

Table 4
Main particulars of the three considered ships for Case study 2.

	M510A/M510B		PSVH		
	Full scale	Model 1:42	Full scale	Model 1:42[a]	
Length overall, L_{oa}	79.80	1.900	53.30	1.269	[m]
Length between perpendiculars, L_{pp}	69.30	1.650	50.69	1.207	[m]
Breadth middle, B	18.02	0.429	11.38	0.271	[m]
Draught, T	4.83	0.115	3.95	0.094	[m]
Displacement, Δ	4103.10	0.05371	1687.09	0.02208	[t]
Block coefficient, C_B	0.664	0.660	0.687	0.683	[-]

[a]The PSVH model was made in scale 1:70, while the M510 models were in scale 1:42. For the tests with three ships, the scale 1:42 was adopted. The numerical transfer functions for PSVH obtained in WAMIT were in scale 1:70; they had to be converted to the new scale 1:42 using Froude scaling.

Table 5
Experimental conditions for Case study 2, in terms of the relative wave heading and generating sea state in the wave tank. The vessels have zero forward speed.

Scenario nr.	Sea state			M510A	M510B	PSVH
	H_s [m]	T_p [s]	γ [-]	β [°]	β [°]	β [°]
D	1.2	8.0	3.3	140	210	160
E	1.5	12.0	3.3	140	210	160

of the vessels can be visualized. The wave tank has 148 active flaps distributed on the four sides that act as an active beach, to avoid wave reflection at the walls (de Mello et al., 2013). Additionally, three wave probes ("WP") recorded the wave elevation time series during the whole process, at three locations in the tank; see the drawing in Fig. 14.

In everything that follows, all quantities are given in full scale, that is after applying a Froude scaling (1:42) to the frequencies, wave period, significant wave height, RAOs and responses. This facilitates the analysis, in view of the results from the previous Case study 1.

5.2. Experimental data verification and validity of stationary conditions

The validity of the assumption of stationary and homogeneous wave conditions in the tank is checked by inspecting the power spectral density (PSD) of the wave elevation measured by WP1, WP2 and WP3, and comparing them to the generating (expected) JONSWAP wave spectrum. This is shown in Fig. 15 for scenarios D and E. All time series (wave elevation and responses) have been trimmed at the beginning (minus 2000 s, full-scale) and the end (minus 1277 s) of the run to avoid transient effects; the remaining length is 3600 s = 1 h. The PSDs are computed by Welch's method of time-average of short modified periodograms (Welch, 1967), which is implemented e.g. in the `scipy.signal.csd` function[3] available in Python's module dedicated to signal processing. It is observed from Fig. 15 that the PSDs from the three wave probes are in good agreement with each other, and satisfactorily coincide with the generating spectrum, both in terms of the peak frequencies and the PSD distributions. Consequently, it is reasonable to assume that the three ships experience – in a statistical sense – the same sea state. It may be noted that the PSD at the peak is a bit lower than expected, which might be caused by the wave maker not providing the specified energy at the peak, or due to some energy dissipation in the tank.

To more accurately know what the wave systems encountered by the ships are, it would ideally be needed to probe the wave elevation in the vicinity of the vessels. This is difficult to do in practice, and such data was unavailable for these experimental datasets. The performed check for homogeneous conditions is therefore quite rough, albeit a necessary one. One should remain aware of the fact that the responses might be impacted by ship-to-ship interactions. This especially concerns vessel M510A, which is located in a sheltered area, downstream of PSVH. M510B is probably less affected by interaction effects than M510A. To the authors' knowledge, there was no possible way to verify these hypotheses, due to the absence of data on the forces and moments experimented by the ships; thus, great care is required in the interpretation of the test results. Using a larger basin would allow for more distance between the ships to reduce the ship-to-ship interactions. Or, in a more time-consuming manner, one could make a separate run for each ship model alone, placed at its respective position, using the same wave realization for each tested vessel.

5.3. Results and discussions for Case study 2

To make sure that the sea state estimates are compared to the actual wave conditions in the tank, the measurements from one arbitrarily selected wave probe (WP1) are used in the following as a basis for comparison, rather than the theoretical JONSWAP spectrum. It is stressed, however, that the spectrum of WP1 is nothing more than a good *estimate* of the ground-true spectrum at the exact location of the particular ship.

[3] A Parzen window is used and the length of the segments is set to 2^{11} = 2048 points, including an overlap of 1024 points between segments.

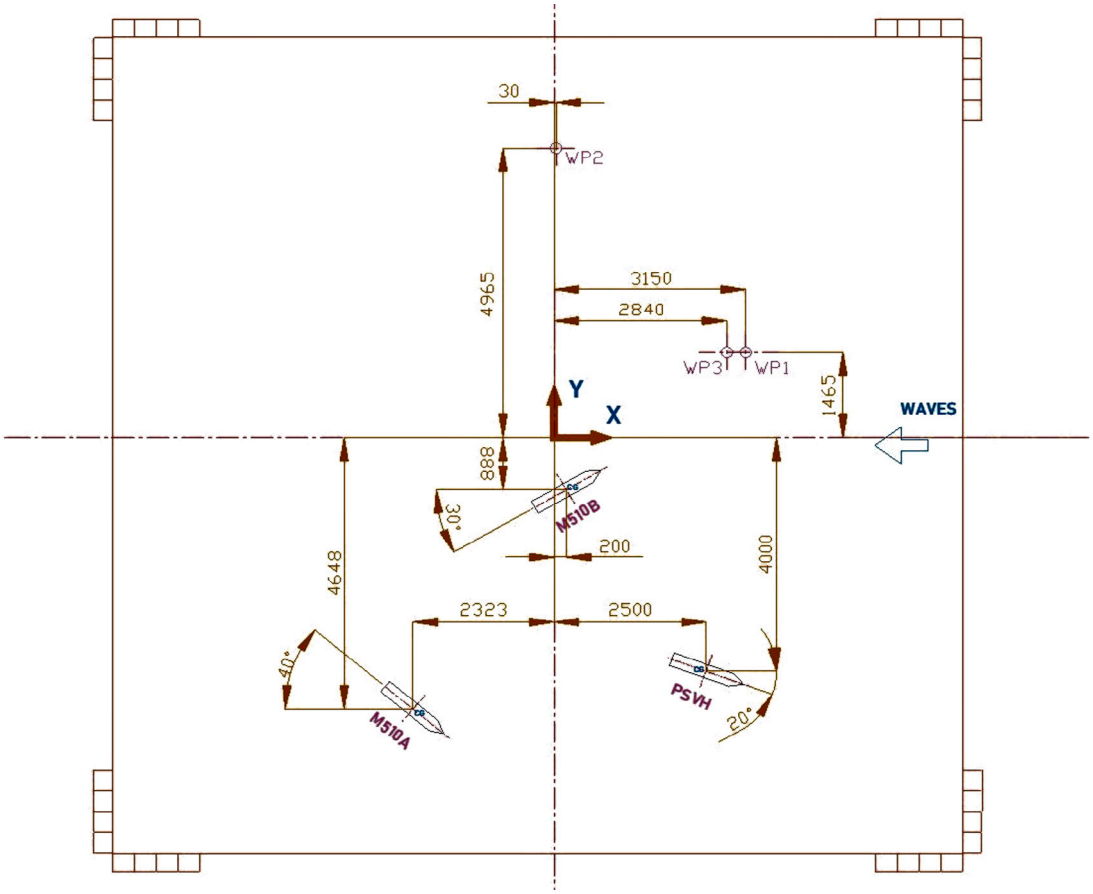

Fig. 14. Drawing of the experimental set-up at the CH-TPN Wave Tank facility. Note that those are model-scale dimensions.

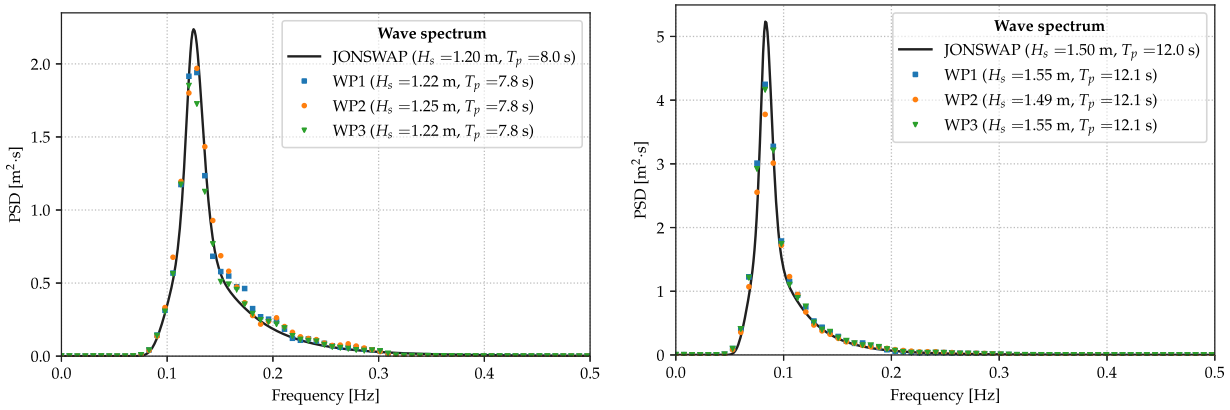

(a) Scenario D (b) Scenario E

Fig. 15. Power spectral density of the wave elevation measured by wave probes WP1 to WP3 and generating JONSWAP wave spectrum for the two scenarios of Case study 2.

Appendix B includes a plot of the ship-specific estimates before and after the RAO-tuning step for scenario D. The plot for scenario E is given in Fig. 16.

The weighted wave spectra are shown in Fig. 17 for the two scenarios, before and after tuning of the RAOs. The arithmetic mean-based weighting was again chosen, like in Case study 1. Here, the beneficial effect of tuning the RAOs is less evident, compared to the results from Case study 1. In scenario D, the agreement is slightly better using the tuned RAOs, rather than the original CFE. In scenario E, the first sea state estimate agrees fairly well with the generating wave spectrum,

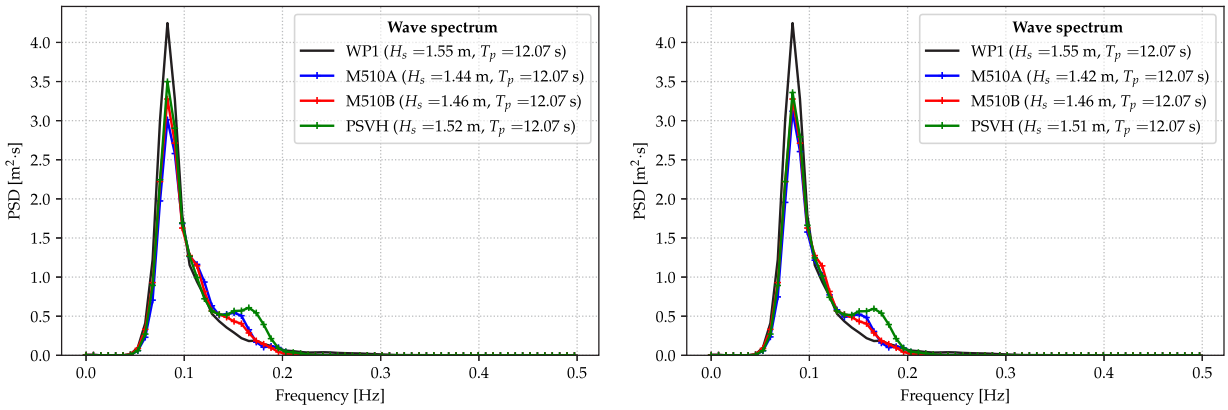

(a) Using *original* closed-form RAOs (b) Using *tuned* closed-form RAOs

Fig. 16. Measured and estimated wave spectra from the three ships in scenario E of Case study 2.

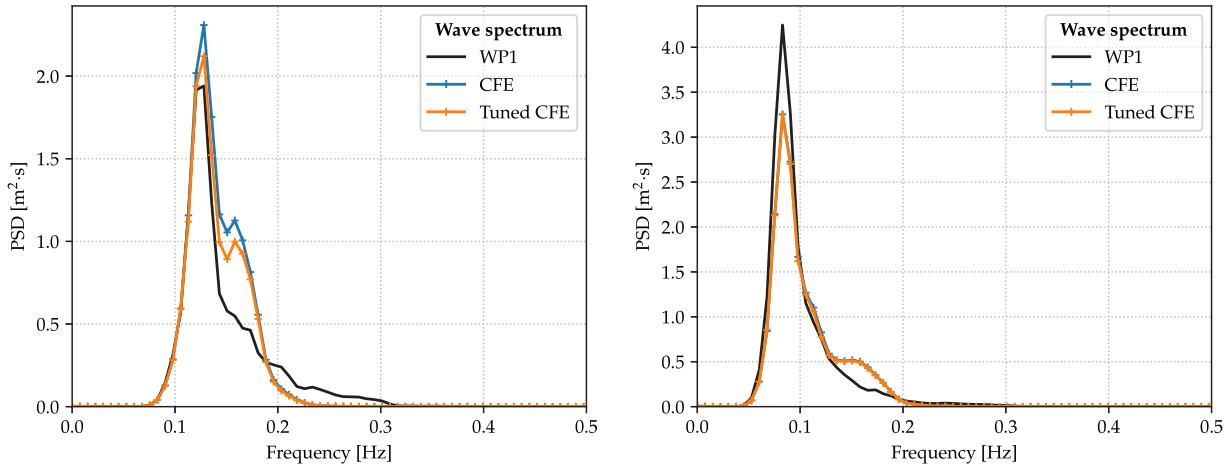

(a) Scenario D (b) Scenario E

Fig. 17. Weighted wave spectra from the three ships in Case study 2. The solid lines represent the PSD of wave elevation recorded by a wave probe (WP1), while the lines with plus markers correspond to estimates in the WBA framework. "CFE" refers to the estimate before tuning the RAOs, that is using the original closed-form expressions, while "Tuned CFE" uses the tuned RAOs.

and therefore, the wave spectrum estimate is almost unchanged by using the tuned RAOs.

The transfer functions used to obtain the sea state estimates are plotted in Figs. 18 and 19. For scenario D, the majority of the tuned RAOs match better the WAMIT RAOs, compared to the original CFE. For scenario E, the tuned RAOs are pretty much similar to the original CFE. To explain this, it is observed from Fig. 16-(a) that the wave spectrum estimates for all ships agree with each other; they are precise sea state estimates. This is also reflected in the uncertainty measure Ψ, see Fig. 20, which does not change much over the iterations. It is simply the best estimate of the RAOs and sea state one can obtain with these three ships in this scenario. One may get incrementally better estimates by adjusting the parameters in the algorithms (gains, tolerances, bounds on the tuning coefficient, etc.). It is emphasized that the parameter values for the RAO-tuning step have not been changed from Case study 1 to Case study 2.

The evolution of the integral-form uncertainty measure over a larger number of iterations is shown in Fig. 20 for the two scenarios. The same findings as in Case study 1 apply here, namely a significant decrease of the relative uncertainty after iteration 1 and a somewhat oscillatory behaviour in the next iterations, particularly noticeable in scenario D.

Similarly to what was presented in Case study 1, the main results from Case study 2 are gathered in Table 6, in terms of estimated sea state parameters and integral uncertainty, obtained at the end of iterations 0, 1, and 4.

Table 6
Results from Case study 2, at the end of iterations 0, 1, and 4.

Scenario	H_s [m]			T_p [s]			Ψ [-]		
	0	1	4	0	1	4	0	1	4
D	1.33	1.28	1.27	7.81	7.81	7.81	0.139	0.101	0.137
E	1.48	1.47	1.45	12.07	12.07	12.07	0.085	0.072	0.072

6. General discussions on the performance of Algorithm 1

The performance of the whole architecture is very sensitive to the values given to the parameters for both the SSE step and RAO-tuning (tolerances, optimization bounds, maximum number of iterations, etc.). Finding the right values for those parameters is viewed as the biggest challenge of the proposed computational architecture.

The possible issue of having a systematic bias at higher frequencies in the CFEs was raised in Section 4.1. In fact, the chosen RAO-tuning method presents the disadvantage that it can only correct the RAOs at observed frequencies, i.e. at the frequencies of non-zero amplitude. There will therefore be no effect of tuning at unobserved frequencies.

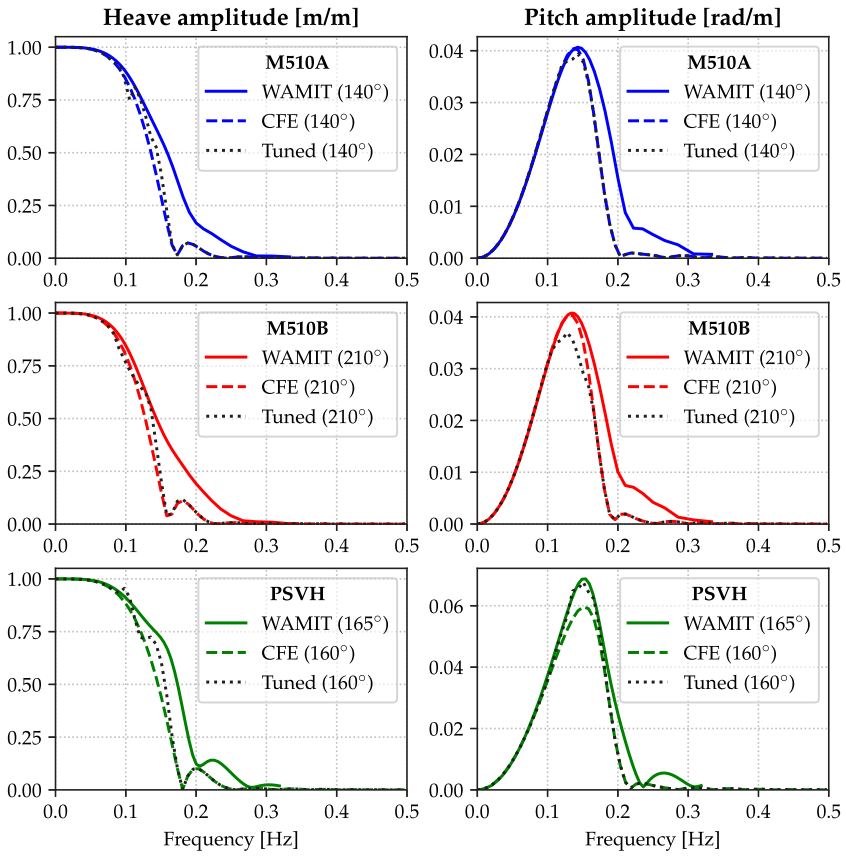

Fig. 18. Heave and pitch RAOs of the three ships in scenario D of Case study 2. The solid lines represent the theoretical RAOs obtained from a linear potential flow theory-based panel code (WAMIT), the dashed lines correspond to the closed form (CFE) solutions given in Jensen et al. (2004), and the black dotted lines are the tuned RAO estimates obtained at the end of the first iteration.

This is an issue, in connection with the use of CFEs, because the higher-frequency bias cannot be properly corrected, resulting in tuned RAOs that still decline too soon towards higher frequencies. This bias has repercussions on the sea state estimates obtained by the wave buoy analogy. Such an effect is amplified by the fact that a non-parametric method was chosen for the SSE step. Indeed, the systematic bias of the sea state estimates could be mitigated by imposing a predefined (realistic) shape of the wave spectrum, for instance, a parameterized JONSWAP wave spectrum, which, on the other hand, could introduce different types of inconsistencies. Alternatively, one could use a parametric method for the RAO-tuning step, e.g. Nielsen et al. (2022), where some of the input parameters of the CFEs are optimized to reduce the systematic bias. It is noted that the network-based approach is beneficial to mitigate the bias in the weighted sea state estimates, considering the multiple ships in the network as low-pass filters with different cut-off frequencies. To investigate the effect of biased versus unbiased original RAOs, it has been tried in Case Study 2 to use the WAMIT RAOs (instead of the CFEs) in the algorithm. The produced sea state estimates before and after tuning are shown in Fig. 21, which can be compared to Fig. 17. It is seen in Scenarios D and E that the WAMIT RAOs enable a better agreement with the WP1 spectrum (compared to the CFEs) in the range of frequencies [0.14–0.18] Hz. However, it is also noticed in Scenario E that neither the original nor the tuned RAOs enable an accurate estimation of the peak amplitude, as was already observed in Fig. 17 for the CFE RAOs. This could be due to an issue with the measured responses in the experiments, possibly caused by some unwanted effects in the experimental set-up, such as ship-to-ship interaction. However, it must be emphasized that the WAMIT RAOs should also be attached some sort of uncertainty and might as well be biased at the peak.

In the occurrence of nonlinear and/or coupled measured responses, it is expected that the effectiveness of the scheme would not be significantly impacted, since the algorithm would still be able to tune the RAOs. However, substantial variations would appear in the tuned RAOs from one time window to the next, indicating the capture of second- and possibly higher-order effects.

When the computational cost of the presented numerical procedure is analysed, the functions `ComputeSSE` and `TuneRAO_R`, referring back to Algorithm 1, should be optimized to run as fast as possible. In this way, frequent updates of the (aggregated) sea state estimate are facilitated in a near real-time set-up. This will meet the ship operators' needs in the event of quickly changing operational and/or environmental conditions. The specific implementation of the SSE step used in the two case studies is extremely fast, whereas the RAO-tuning process – which relies on an optimization procedure – represents the most time-consuming step. One easy way to reduce the computational time of the RAO-tuning step would be to reduce the number of tuning coefficients for which the optimization problem is to be solved. In Case study 1, the spectra are discretized in 100 frequency components in the RAOs, which leads to 100 tuning coefficients. It is possible to work with a lower resolution in practical engineering applications, especially to enable more frequent updates of the sea state estimates when online SSE is regarded. However, the results (not presented in this paper) from running the algorithm in Case study 1 with less (50) frequency components showed that the accuracy of the estimates was quite drastically reduced in two out of three scenarios, while the precision was not significantly impacted by the change in any of the scenarios.

Another important aspect of the network-based procedure is the configuration of the ships, and especially their headings relative to the incoming waves. It was observed that the latter has a significant effect

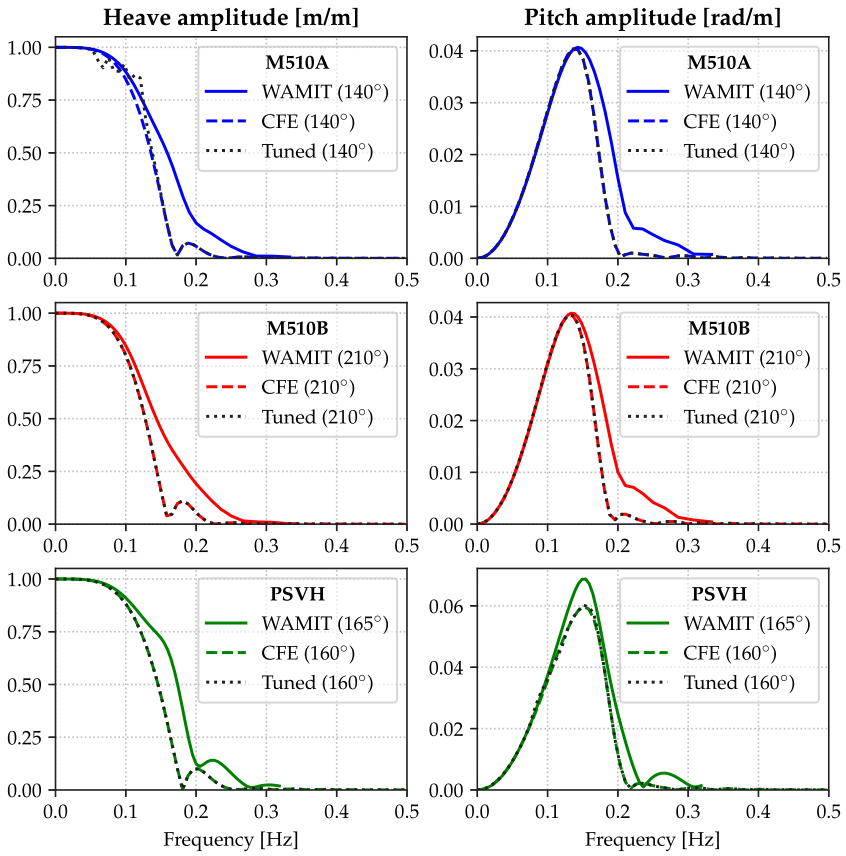

Fig. 19. Heave and pitch RAOs of the three ships in scenario E of Case study 2.

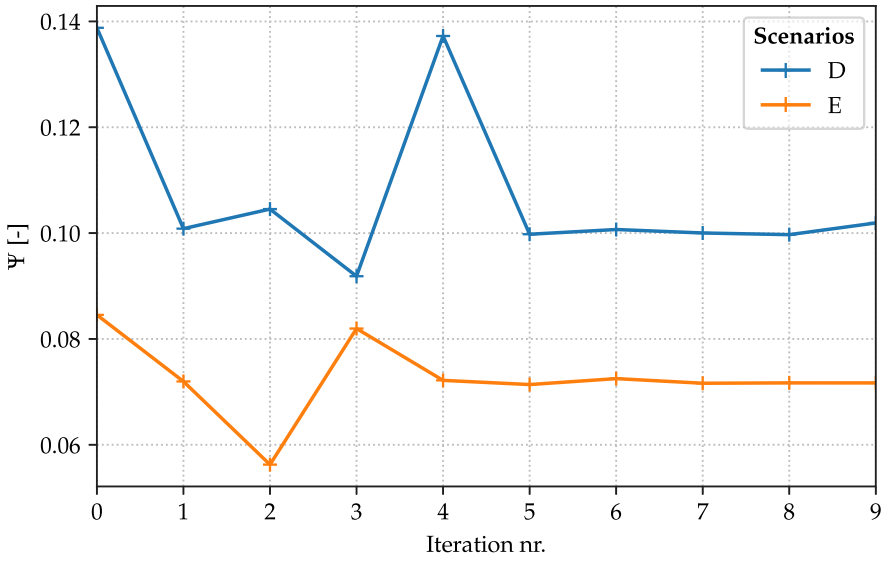

Fig. 20. Uncertainty measure versus number of iterations, for the two scenarios of Case study 2.

on the performance of the proposed method. This was verified through Case study 1. Although the results are, for the sake of conciseness of the paper, not shown here, a few additional scenarios were considered, where the three ships had the same relative heading. Three values were tried for β, namely 100°, 130° and 160°, resulting in poorer performances of the algorithm compared to scenarios A, B, and C, both in terms of stability and ability to provide more accurate sea state estimates after a few iterations. This can be explained by the fact that the relative wave heading influences the range of frequency at which the ship has a non-zero response, that is the ship's bandwidth. Remembering that the single vessel acts as a linear filter with particular characteristics on the incoming waves, it is beneficial to work with a group of ships having a large bandwidth, when a network of wave recorder systems is considered, as this is favourable for the estimation capabilities.

Another noteworthy point is the interdependency inherently built into the architecture. Hereby, it is understood that the procedure is repeated in several iterations, which means that more and more

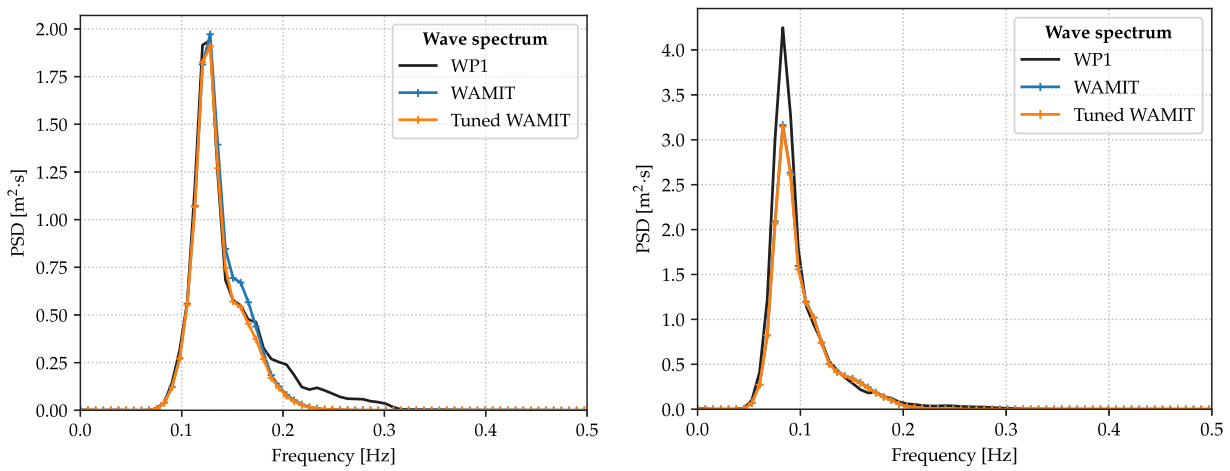

Fig. 21. Weighted wave spectra from the three ships in Case study 2. The solid lines represent the PSD of wave elevation recorded by a wave probe (WP1), while the lines with plus markers correspond to estimates in the WBA framework. "WAMIT" refers to the estimate using the original WAMIT RAOs, while "Tuned WAMIT" uses the tuned WAMIT RAOs.

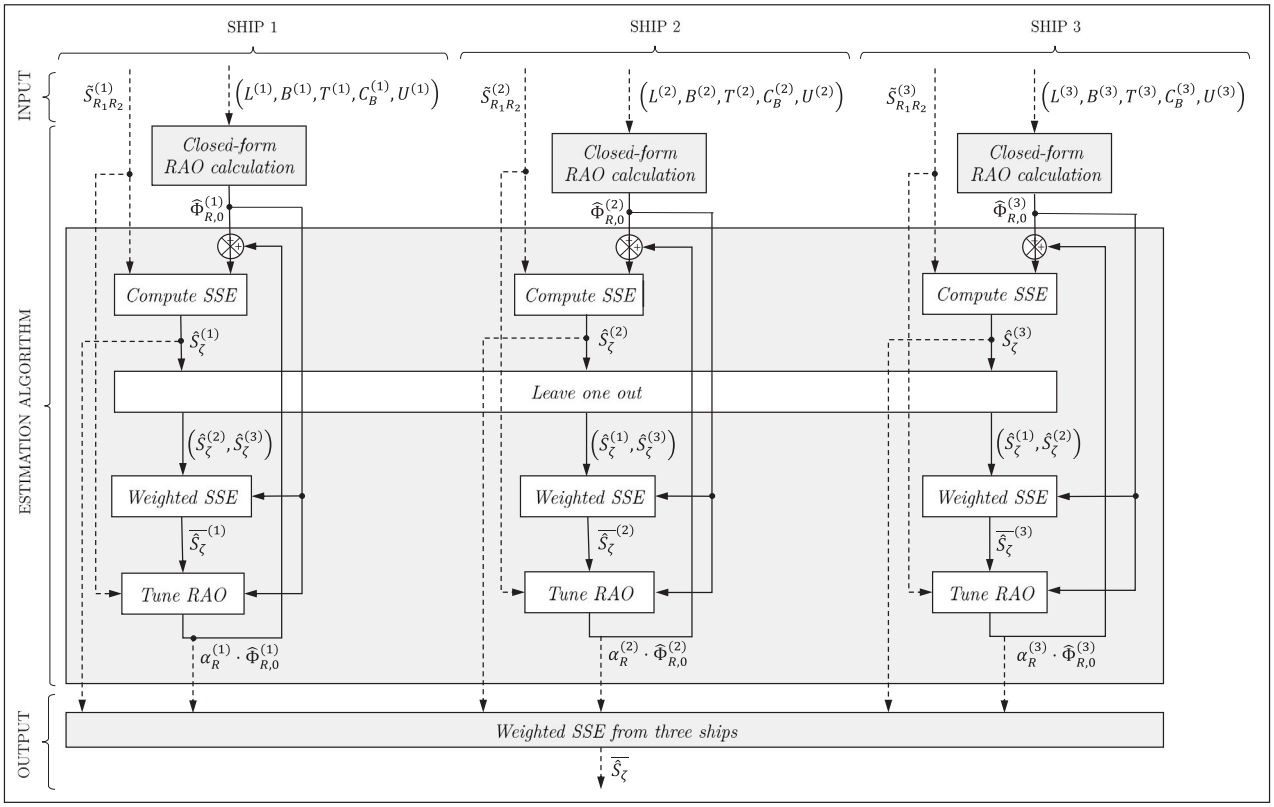

Fig. A.22. Illustration of Algorithm 1 applied to a network of three ships.

interdependency between the two steps (RAO-tuning and SSE) builds up in the outputs. This can have unwanted effects if the algorithm enters a vicious circle, in which errors propagate and accumulate from one step to the other. For example, if the initial RAO estimate is bad over a range of frequencies, then the quality of the produced sea state estimate can be as well impacted in that range, which, in turn, degrades the RAOs even more after tuning, due to imprecision in the sea state description; and so forth. From Figs. 11, 12 and 20, it can be argued that stopping the process after the first iteration is the most reasonable recommendation, for robustness, accuracy and precision of the sea state estimate. This practical choice results in tuning the RAOs once only, and in subsequently producing a new sea state estimate, using these tuned RAOs. Nevertheless, only five test scenarios have been considered in the present study, which is hardly sufficient to build strong evidence that one iteration is necessarily the best practice. This hypothesis should be validated against some additional test cases, which are left for future work.

7. Concluding remarks and future work

The paper presented a novel concept for estimating the sea state encountered by a network of ships operating in dynamic positioning in

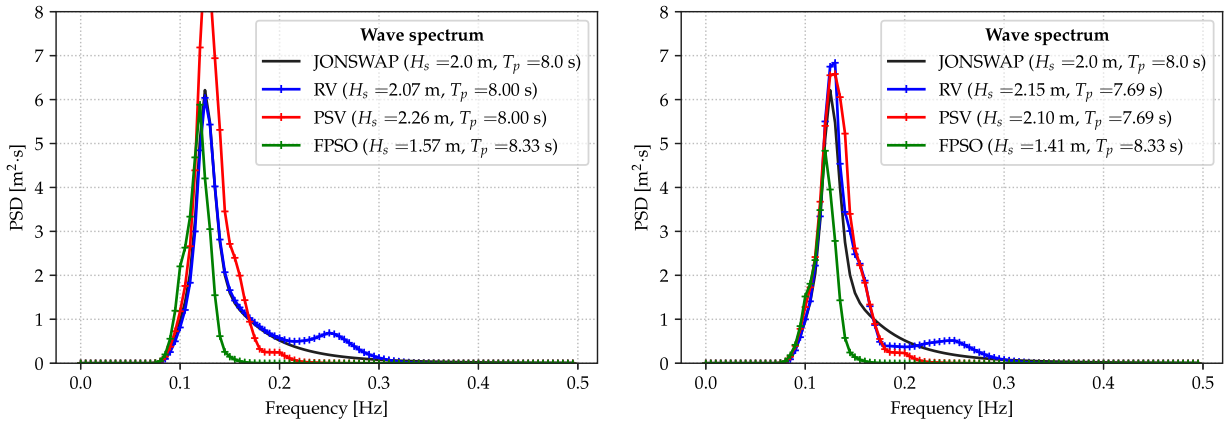

(a) Using *original* closed-form RAOs (b) Using *tuned* closed-form RAOs

Fig. B.23. Exact and estimated wave spectra from the three ships selected for scenario A of Case study 1. Left: estimates before any tuning of the RAOs, that is using the original closed-form expression; Right: estimates using the tuned RAOs.

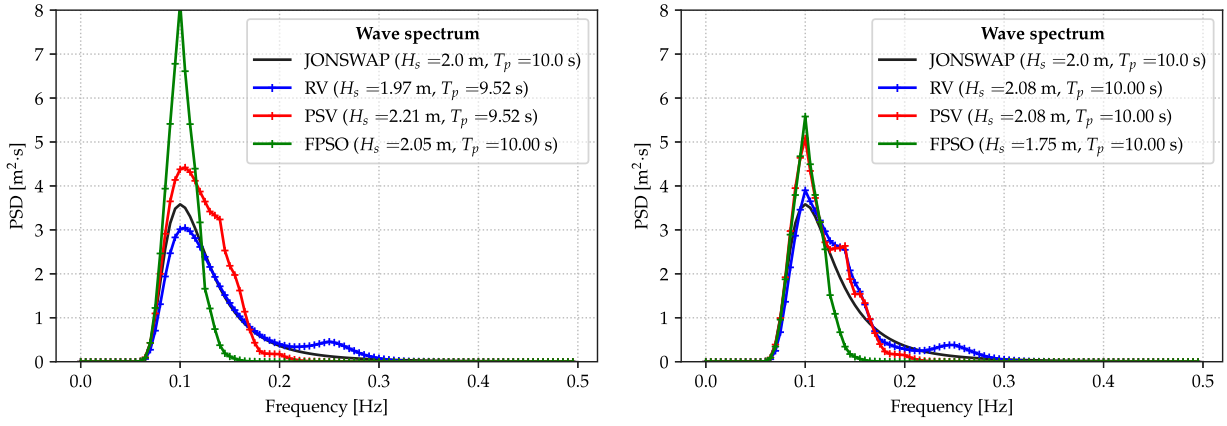

(a) Using *original* closed-form RAOs (b) Using *tuned* closed-form RAOs

Fig. B.24. Exact and estimated wave spectra from the three ships in scenario B of Case study 1.

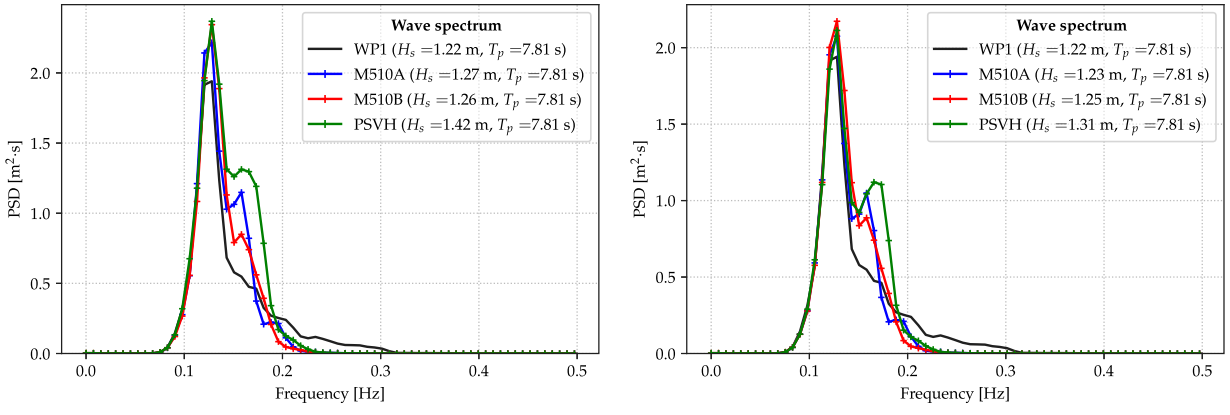

(a) Using *original* closed-form RAOs (b) Using *tuned* closed-form RAOs

Fig. B.25. Measured and estimated wave spectra from the three ships in scenario D of Case study 2.

the same geographical area. Tuning of the vessels' response amplitude operators is performed simultaneously to sea state estimation, in a "leave-one-out" fashion — that is considering only the sea state estimates from all the *other* ships in the network when trying to tune one ship's response amplitude operators. In addition to an initial estimate of the response amplitude operators, the proposed algorithm only needs measured vessel motion cross-spectra as input. The procedure was tested through two case studies, one based on simulated ship motions, and the other using experimental data from model-scale tests in a wave tank. In total, five different scenarios in unimodal, long-crested waves were analysed, and they showed that the proposed algorithm is able to produce accurate estimates of the 1-D wave spectrum. What is more,

the trials revealed that in some cases, the tuning of the RAOs can significantly reduce the uncertainty of the wave spectrum estimates, which also comes with some improvement in accuracy, compared to the estimates without tuning.

Many simplifications and assumptions were made in this conceptual study. In particular, in Case study 1, the computations have been carried out in the frequency domain, without generating any realization of vessel motion time histories. Instead, the simulated motion spectra have been used directly as input to Algorithm 1. This is not realistic, since measurement noise and sampling uncertainty would affect the quality of the motion spectra in real life. However, this choice was motivated by the need to keep the simulation as simple as possible to make it easier to study the performance of the proposed algorithm. That is also why the algorithm was then tested in a second case study with real data from model experiments.

Furthermore, it would be interesting to make a sensitivity study of the number of ships in the network. As pointed out in the discussions, the sizes of the ships compared to the waves and the relative headings are also important factors to be studied. More model-scale experimental results and (full-scale) in-service data will be needed in the future to investigate the potential of network-based methods for real-time sea state estimation and prediction.

The overall architecture, as illustrated by Algorithm 1, is generic and modular in essence, meaning that it is compatible with various methods for the SSE and RAO-tuning steps. Very important for the full applicability of the method, the case of multimodal short-crested seas – where wind waves coexist with one or more swell systems – requires consideration in a necessary extension of the proposed simultaneous RAO-tuning and SSE framework. The directional wave spectrum is the fundamental quantity of wave modelling and the quantity that allows calculating the consequences of interactions between waves and other matter (Hauser et al., 2005). Bayesian modelling, see e.g. Iseki and Ohtsu (2000), is specially adapted to solve for 2-D wave spectra, and forward speed effects can be included by accounting for the Doppler shift. Considering the large number of ships sailing in the world's oceans and seas, the overarching aim is to test the method eventually in a network of in-service vessels with advance speeds, regarded as sailing wave buoys. Parenthetically, possible fluctuations of the ships' heading and speed should be appropriately handled to ensure that the spectral calculations are made over time windows of stationary conditions. The network could also comprehend several smaller drone vessels (Dallolio et al., 2021), moored "classical" wave-buoys, or shipborne wave radars. Overall, such a network of in-situ wave recorders should be able to frequently provide updated estimates of the encountered sea state, (ideally) immediately available to the operators during operations at sea. Shipping companies need reliable wave estimates, as well as forecasts, at the actual positions of the fleet of ships to make calculations of the added wave resistance and, consequently, more qualified evaluations of the fuel consumption performance on the specific sea routes; see e.g. Prpic-Oršic et al. (2018).

CRediT authorship contribution statement

Raphaël E.G. Mounet: Conceptualization, Methodology, Software, Formal analysis, Investigation, Writing, Visualization. **Ulrik D. Nielsen:** Methodology, Software, Investigation, Writing, Visualization, Supervision, Project administration. **Astrid H. Brodtkorb:** Methodology, Software, Investigation, Writing, Visualization, Supervision. **Eduardo A. Tannuri:** Investigation, Resources. **Pedro C. de Mello:** Investigation, Resources, Data curation.

Declaration of competing interest

The authors declare that they have no known competing financial interests or personal relationships that could have appeared to influence the work reported in this paper.

Data availability

The data that has been used is confidential.

Acknowledgements

This work was supported by the Research Council of Norway through the Centres of Excellence funding scheme [project number 223254 AMOS]. Moreover, the financial support from The Danish Maritime Fund [case numbers 2017–101 and 2020–074] is greatly acknowledged. The academic experiments used for Case study 2 were conducted by Mello, P.C. and Ianagui, A.S.S.

Appendix A. Main algorithm

Algorithm 1 is presented in a general manner, to make it applicable to a wide range of practical situations, e.g. with short-crested waves and/or non-zero vessel forward speed.

In the algorithm, iterations of the SSE (or `ComputeSSE(...)`) and RAO-tuning (or `TuneRAO_R(...)`) steps are repeated until the stopping criterion defined by the function `StopLoop(...)` is reached. A priori, there could be several possible options for a suitable stopping criterion – with different input parameters for the `StopLoop` function – for instance: (1) to stop the process when the RAO estimate does not vary anymore (below a set threshold) for all ships, (2) to stop when the uncertainty of the sea state estimates has been sufficiently reduced, or (3) to set a maximum number of iterations. In this study, option (3) is selected, which turns the "While" loop into a "For" loop, more convenient when it comes to comparing different test cases.

It is emphasized that, regardless of the iteration number, the RAO-tuning step always takes the original closed-form expression of the RAOs as input, i.e. its initial version from iteration 0, whereas the SSE step uses the tuned RAOs, meaning that it works with the latest version of the RAOs. The fundamental reasoning behind this distinction is that, when fitting the tuning coefficients α_R, it makes little physical sense to use as an initial guess the coefficient values that were obtained in a previous iteration, because those are related to an old and deprecated sea state estimate. Resetting the coefficients α_R to zero after each new iteration limits the propagation of errors in the tuned RAOs from one iteration to the next one, as this approach avoids – at least to some extent – an unwanted interdependency between successive RAO estimates.

The use of Algorithm 1 in practice in a network of three ships

In Sections 4 and 5, the algorithm is demonstrated in two case studies, in both of which three ships are considered in the network for SSE. Then, to better visualize the input–output relationships and the leave-one-out principle, Fig. A.22 illustrates the procedure for the specific network configuration.

Appendix B. Individual ship-specific sea state estimates

The ship-specific wave spectrum estimates for scenarios A, B, and D are plotted in Figs. B.23, B.24, and B.25, respectively. For scenarios C and E, the estimates have already been presented in Figs. 7 and 16, Sections 4.2 and 5.3, respectively.

Algorithm 1: SSE with leave-one-out tuning of transfer functions for multiple ships

Input : N, $\{L^{(n)}, B^{(n)}, T^{(n)}, C_B^{(n)}, U^{(n)}\}_{n=1\dots N}$, $\left\{\left\{\tilde{\mathbf{S}}_{RR}^{(n)}\right\}_{R\in\mathcal{R}^{(n)}}\right\}_{n=1\dots N}$

Output: $\left\{\hat{\mathbf{S}}_{\zeta}^{(n)}\right\}_{n=1\dots N}$, $\left\{\left\{\hat{\mathbf{\Phi}}_{R}^{(n)}\right\}_{R\in\mathcal{R}^{(n)}}\right\}_{n=1\dots N}$

/* Initialization of the transfer functions with closed-form expressions. */
for $n \leftarrow 1$ **to** N **do**
  for $R \in \mathcal{R}^{(n)}$ **do**
    $\hat{\mathbf{\Phi}}_{R,0}^{(n)} \leftarrow$ ClosedFormSol_R$(L^{(n)}, B^{(n)}, T^{(n)}, C_B^{(n)}, U^{(n)})$
  end for
end for
$SSE\_Found \leftarrow False$
$m \leftarrow 0$
while *SSE_Found is False* **do**
  $m \leftarrow m + 1$
  for $n \leftarrow 1$ **to** N **do**
    /* Sea state estimation step. */
    $\hat{\mathbf{S}}_{\zeta,m}^{(n)} \leftarrow$ ComputeSSE$(\left\{\hat{\mathbf{\Phi}}_{R,m-1}^{(n)}\right\}_{R\in\mathcal{R}^{(n)}}, \left\{\tilde{\mathbf{S}}_{RR}^{(n)}\right\}_{R\in\mathcal{R}^{(n)}})$
  end for
  for $n \leftarrow 1$ **to** N **do**
    /* RAO-tuning step. */
    $\bar{\hat{\mathbf{S}}}_{\zeta,m}^{(n)} \leftarrow$ WeightedSSE$(\left\{\hat{\mathbf{S}}_{\zeta,m}^{(p)}\right\}_{p\in\{1\dots N\}\setminus n})$
    for $R \in \mathcal{R}^{(n)}$ **do**
      $\hat{\mathbf{\Phi}}_{R,m}^{(n)} \leftarrow$ TuneRAO_R$(\bar{\hat{\mathbf{S}}}_{\zeta,m}^{(n)}, \hat{\mathbf{\Phi}}_{R,0}^{(n)}, \tilde{\mathbf{S}}_{RR}^{(n)})$
    end for
  end for
  /* Check for the stopping criterion. */
  if $StopLoop(...)$ **then**
    $SSE\_Found \leftarrow True$
  end if
end while
return $\left\{\hat{\mathbf{S}}_{\zeta,m}^{(n)}\right\}_{n=1\dots N}$, $\left\{\left\{\hat{\mathbf{\Phi}}_{R,m}^{(n)}\right\}_{R\in\mathcal{R}^{(n)}}\right\}_{n=1\dots N}$

References

Bitner-Gregersen, E.M., Bhattacharya, S.K., Chatjigeorgiou, I.K., Eames, I., Ellermann, K., Ewans, K., Hermanski, G., Johnson, M.C., Ma, N., Maisondieu, C., Nilva, A., Rychlik, I., Waseda, T., 2014. Recent developments of ocean environmental description with focus on uncertainties. Ocean Eng. 86, 26–46. http://dx.doi.org/10.1016/j.oceaneng.2014.03.002.

Brodtkorb, A.H., Nielsen, U.D., J. Sørensen, A., 2018a. Online wave estimation using vessel motion measurements. IFAC-PapersOnLine 51 (29), 244–249. http://dx.doi.org/10.1016/j.ifacol.2018.09.510.

Brodtkorb, A.H., Nielsen, U.D., J. Sørensen, A., 2018b. Sea state estimation using vessel response in dynamic positioning. Appl. Ocean Res. 70, 76–86. http://dx.doi.org/10.1016/j.apor.2017.09.005.

Byrd, R.H., Hribar, M.E., Nocedal, J., 1999. An interior point algorithm for large-scale nonlinear programming. Siam J. Optim. 9 (4), 877–900. http://dx.doi.org/10.1137/S1052623497325107.

Dallolio, A., Quintana-Diaz, G., Honoré-Livermore, E., Garrett, J.L., Birkeland, R., Johansen, T.A., 2021. A satellite-USV system for persistent observation of mesoscale oceanographic phenomena. Remote Sens. 13 (16), 3229. http://dx.doi.org/10.3390/rs13163229.

de Mello, P.C., Carneiro, M.L., Tannuri, E.A., Kassab, F., Marques, R.P., Adamowski, J.C., Nishimoto, K., 2013. A control and automation system for wave basins. Mechatron. 23 (1), 94–107. http://dx.doi.org/10.1016/j.mechatronics.2012.11.004.

Han, X., Leira, B.J., Sævik, S., 2021a. Vessel hydrodynamic model tuning by discrete Bayesian updating using simulated onboard sensor data. Ocean Eng. 220, 108407. http://dx.doi.org/10.1016/j.oceaneng.2020.108407.

Han, X., Leira, B.J., Sævik, S., Ren, Z., 2021b. Onboard tuning of vessel seakeeping model parameters and sea state characteristics. Mar. Struct. 78, 102998. http://dx.doi.org/10.1016/j.marstruc.2021.102998.

Hasselmann, K., et al., 1973. Measurements of Wind-Wave Growth and Swell Decay During the Joint North Sea Wave Project (JONSWAP). (12), Deutschen Hydro-graphischen Institut, Reihe A, Hamburg, Germany.

Hauser, D., Kahma, K., Krogstad, H.E., Lehner, S., Monbaliu, J.A.J., Wyatt, L.R., 2005. Measuring and analysing the directional spectra of ocean waves. EU COST Action 714.

Iseki, T., Ohtsu, K., 2000. Bayesian estimation of directional wave spectra based on ship motions. Control Eng. Pract. 8 (2), 215–219. http://dx.doi.org/10.1016/S0967-0661(99)00156-2.

Jensen, J.J., 2001. Load and Global Response of Ships. In: Elsevier Ocean Engineering Book Series, Vol. 4, Elsevier.

Jensen, J.J., Mansour, A.E., Olsen, A.S., 2004. Estimation of ship motions using closed-form expressions. Ocean Eng. 31 (1), 61–85. http://dx.doi.org/10.1016/S0029-8018(03)00108-2.

Kaasen, K.E., Berget, K., Lie, H., Bjørkli, R., 2020. Automatic tuning of vessel models offshore: A feasibility study using high-precision data from model test. Proc. Annu. Offshore Technol. Conf. 2020, http://dx.doi.org/10.4043/30690-MS.

Lloyd, A.R.M.J., 1998. Seakeeping, second ed. Ellis Horwood.

Montazeri, N., 2016. Estimation of Waves and Ship Responses using Onboard Measurements. In: Doctoral thesis at DTU, Technical University of Denmark, Department of Mechanical Engineering, Kgs. Lyngby.

Nielsen, U.D., 2017. A concise account of techniques available for shipboard sea state estimation. Ocean Eng. 129, 352–362. http://dx.doi.org/10.1016/j.oceaneng.2016.11.035.

Nielsen, U.D., 2021. Spatio-temporal variation in sea state parameters along virtual ship route paths. J. Oper. Oceanogr. 1–18. http://dx.doi.org/10.1080/1755876X.2021.1872894.

Nielsen, U.D., H. Brodtkorb, A., J. Sørensen, A., 2019. Sea state estimation using multiple ships simultaneously as sailing wave buoys. Appl. Ocean Res. 83, 65–76. http://dx.doi.org/10.1016/j.apor.2018.12.004.

Nielsen, U.D., Ikonomakis, A., 2021. Wave conditions encountered by ships—A report from a larger shipping company based on ERA5. Ocean Eng. 237, 109584. http://dx.doi.org/10.1016/j.oceaneng.2021.109584.

Nielsen, U.D., Mounet, R.E.G., Brodtkorb, A.H., 2021. Tuning of transfer functions for analysis of wave-ship interactions. Mar. Struct. 79, 103029. http://dx.doi.org/10.1016/j.marstruc.2021.103029.

Nielsen, U.D., Mounet, R.E.G., Brodtkorb, A.H., 2022. Parameterised transfer functions with associated confidence bands. Appl. Ocean Res. 125, 103250. http://dx.doi.org/10.1016/j.apor.2022.103250.

Pascoal, R., Guedes Soares, C., 2009. Kalman filtering of vessel motions for ocean wave directional spectrum estimation. Ocean Eng. 36 (6–7), 477–488. http://dx.doi.org/10.1016/j.oceaneng.2009.01.013.

Prpic-Oršic, J., Sasa, K., Valcic, M., Faltinsen, O.M., 2018. Uncertainties of ship speed loss evaluation under real weather conditions. Proc. Intern. Conf. Offshore Mech. Arct. Eng. - OMAE 11B, http://dx.doi.org/10.1115/OMAE2018-78514.

Salvesen, N., Tuck, E.O., Faltinsen, O.M., 1971. Ship Motions and Sea Loads. Vol. 75, 30 s.

Skandali, D., Lourens, E., Ogink, R.H.M., 2020. Calibration of response amplitude operators based on measurements of vessel motions and directional wave spectra. Mar. Struct. 72, 102774. http://dx.doi.org/10.1016/j.marstruc.2020.102774.

St. Denis, M., Pierson Jr., W., 1953. On the motions of ships in confused seas. Trans. SNAME 61, 280–332.

Tannuri, E.A., Sparano, J.V., Simos, A.N., Da Cruz, J.J., 2003. Estimating directional wave spectrum based on stationary ship motion measurements. Appl. Ocean Res. 25 (5), 243–261. http://dx.doi.org/10.1016/j.apor.2004.01.003.

Welch, P.D., 1967. The use of fast Fourier transform for the estimation of power spectra: A method based on time averaging over short, modified periodograms. IEEE Trans. Audio Electroacoust. 15 (2), 70–73.

Yu, C., Xie, L., Verhaegen, M., Chen, J., 2022. Blind Identification of Structured Dynamic Systems: A Deterministic Perspective. Springer Nature, http://dx.doi.org/10.1007/978-981-16-7574-4.

Yuan, Y., Fu, G., Zhang, W., 2016. Extended and unscented Kalman filters for parameter estimation of a hydrodynamic model of vessel. Chin. Control Conf. 2016, 2051–2056. http://dx.doi.org/10.1109/ChiCC.2016.7553668.